Dissertation

submitted to the
Combined Faculties for the Natural Sciences and for Mathematics
of the Ruperto-Carola University of Heidelberg, Germany
for the degree of
Doctor of Natural Sciences

Put forward by
Master of Science Fabian Heiße
Born in Zschopau
Oral examination: October 16$^{\text{th}}$, 2019

High-precision measurement of the proton's atomic mass

First referee: Priv. Doz. Dr. Wolfgang Quint

Second referee: Prof. Dr. Selim Jochim

Groß sind die Werke des HERRN;
wer sie erforscht, der hat Freude daran.

Die Bibel, Buch der Psalmen, Kapitel 111 Vers 2.

Hochpräzise Messung der atomaren Masse des Protons

Zusammenfassung - Im Rahmen dieser Doktorarbeit wurden große Teile des neuen Penningfallen-Experimentes LIONTRAP (Light-Ion Trap) aufgebaut, das gesamte Experiment erstmalig in Betrieb genommen und vollständig charakterisiert. Weiterhin wurden die ersten beiden Messkampagnen zur Bestimmung der atomaren Masse des Protons und des Sauerstoffatoms durchgeführt.
Das LIONTRAP Experiment ist speziell für die Massenbestimmung von leichten Ionen optimiert. Dabei wird die Zyklotronfrequenz eines hochgeladenen Kohlenstoffions mit der des zu messenden Ions verglichen, um über dieses Zyklotronfrequenzverhältnis die atomare Masse des Ions zu extrahieren. Dafür wurde in LIONTRAP die harmonischste zylindrische Penningfalle realisiert, welche bisher in der Literatur beschrieben wurde.
In der ersten Messkampagne wurde die atomare Masse des Protons mit einer bisher unerreichten relativen Genauigkeit von 3×10^{-11} bestimmt. Der neue Messwert ist nicht nur einen Faktor drei genauer als der zum Zeitpunkt der Messung gültige Literaturwert, sondern weist auch eine Diskrepanz von drei Standardabweichungen dazu auf. Zusätzlich wurde auch noch der zweitgenauste Wert für die Sauerstoffmasse bestimmt, welcher mit dem Literaturwert übereinstimmt. Darüber hinaus wurde in einer weiteren Messkampagne ebenfalls der größte systematische Effekt der Protonmassenmessung, der Bildladungseffekt, genau vermessen. Die erreichte relative Genauigkeit von 5% entspricht dabei der zweit genausten Messung dieses Effekts überhaupt. Zusätzlich stimmt das gemessene Ergebnis mit Simulationsvorhersagen überein.

High-precision measurement of the proton's atomic mass

Abstract - In the course of this thesis major parts of the new Penning trap experiment LIONTRAP (Light-Ion Trap) have been built up, the whole apparatus has been commissioned and characterized. This enabled the first two measurement campaigns, including the measurements of the proton's and oxygen's atomic masses.
The LIONTRAP experiment is dedicated to high-precision mass measurements of light ions. The measurement principle is based on the cyclotron frequency comparison of a carbon ion to the one of a light ion to determine its atomic mass. Therefore, the most harmonic cylindrical Penning trap described in the literature so far has been realized.
In the first measurement campaign, the proton's atomic mass has been determined with an unrivaled relative precision of 3×10^{-11}. This result is a factor of three more precise compared to the literature value at this time, revealing a more than three standard deviation to it. Additionally, the oxygen's atomic mass has been measured with the second best precision, in agreement with the literature value. During the second measurement campaign the largest systematic effect of the proton mass measurement, the image charge shift, has been analyzed. The achieved relative uncertainty of 5% is the second most precise measurement reported in literature so far. Moreover, the measured result is in very good accordance with the result predicted by dedicated simulations.

Contents

List of Figures

List of Tables

1 Introduction

1.1 Content of this thesis

One universal and characteristic property of every atomic particle is its rest mass[1]. Masses play a significant role in a lot of areas in our daily lives. Consequently, mass measurements have also been an essential concept in natural sciences right from the early beginning. The masses of particles are important input parameters for theories which describe the fundamental laws of nature. Within the current Standard Model (SM) of particle physics, rest masses are not precisely enough predictable and need to be experimentally measured. On the other hand masses are essential input parameters to test various theories in physics. Furthermore, the predictions of the SM are based on dimensionless constants. Therefore, mass ratios are always required.

In the course of this thesis the new high-precision mass spectrometer LIONTRAP (Light-Ion Trap) has been set up and is presented in detail. This spectrometer enabled us to do the most precise measurement of the proton's atomic mass to date; it has been a factor of three more precise compared to the literature value at this time. In this case the mass of a proton has been compared to the reference mass of a carbon ion.

The thesis starts with an overview of the published proton mass measurements over the last two hundred years, see 1.2. This is followed by the motivation for the LIONTRAP experiment. In chapter 2 the experimental background, the measurement principle as well as an introduction of the image charge effect are presented. The full articles are presented in chapter 3. Chapter 4 discusses the achieved results. In chapter 5 this cumulative thesis is summarized.

1.2 Historical overview of proton mass measurements

In the following chapter I will give a brief overview of the increasing precision of measurements of the proton's mass over the last two centuries, including the major milestones and involved groups. It starts with a relative uncertainty of 10^{-2} in 1814 and reaches uncertainties of 10^{-11} nowadays, see Fig. 1.1.

The combination of a new mass spectrometer and higher precision mass measurements is an always recurring principle in the history of mass metrology. On

[1] In the course of this thesis the term mass always refers to rest mass.

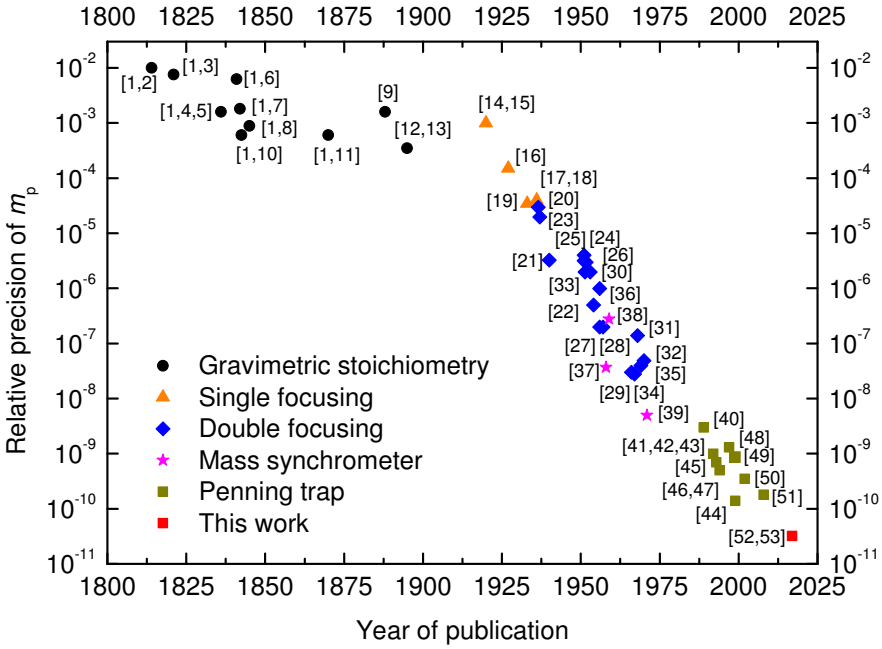

Figure 1.1: Overview of the relative uncertainty for the measurement of the atomic mass of hydrogen, respectively the proton, over the last 200 years. At the beginning the mass was measured using chemical methods [1]. The most important researchers who contributed to the hydrogen mass were Wollaston [2], Berzelius [3], Thomson [4, 5], Dumas [6, 7], Regnault [8] and Richards [9]. The three most precise measurements using chemical methods were conducted by Erdmann [10], Thomsen [11] and Morley [12, 13]. For the first time the mass of hydrogen was measured with a single-focused mass spectrograph by Aston in 1920 [14, 15]. Later he built two improved spectrometers with an enhanced precision [16–18]. Another measurement with a single focused mass spectrometer has been carried out by Bainbridge [19]. From 1936 the application of double-focusing mass spectrometers led to more precise results. At the beginning, measurements with such a device were carried out by the group of Mattauch [20–22] and the group of Bainbridge [23, 24]. Later the groups of Nier [25–29], Ogata [30–32], Ewald [33], Moreland [34, 35] as well as Demirkhanov [36] used similar spectrometers. The next major improvement in precision was based on the application of mass synchrometers by Smith and Christman [37–39]. The invention of Penning traps lead to yet another enhancement by the groups of Van Dyck Jr. [40–44], Pritchard [45–47] and Schuch [48–51]. The most recent measurement was conducted in the course of this thesis with a precision of 3×10^{-11} [52, 53]. On average, every three years a new measurement has been conducted and the precision of the proton mass increases on average by one order of magnitude every 13 years.

the other hand the achieved higher precision results are essential for new insights in fundamental tests in physics. In general, the principle of mass determination is based on the comparison of an unknown mass to a reference mass or mass standard.

Already in the fifth century before Christ the Greek philosophers Leukipp and his scholar Demokrit proposed the concept that all substances are made of undividable pieces. This can also imply that the weight of different substances is an integer multiple of the weight of the lightest substance.

It took until 1803 that the English scientist John Dalton from the University of Manchester developed these first philosophic concepts further and transferred them to physical and chemical ones. He was the first who set the relative atomic mass of hydrogen to 1 [54], since hydrogen was the lightest mass he had found. He set the oxygen's relative mass to 7, carbon to 5.4 and nitrogen to 6 [55]. Due to this achievement, today's atomic mass unit u is also called Dalton (Da) in the field of chemistry.

The discovery of the chemical substance hydrogen itself was first described only a few years earlier by the English scientist Henry Cavendish in 1766 during experiments with metals and acids [56]. However, other researchers have already produced hydrogen hundreds of years earlier, for example Robert Boyle. In 1815 the English chemist William Prout [57, 58] proposed the hypothesis that all substances are built of different integer numbers of hydrogen, which was in conflict with the measurements of Dalton and others.

The law of combining volumes [59], discovered in 1809 by the French scientist Joseph Louis Gay-Lussac from the University of Paris, indicates that for a reaction of gases resulting in another different gas the ratio of the reactant gases to the product gases can be described by a ratio of whole numbers. For example, he found out that two volumes of hydrogen and one volume of oxygen reacts to one volume of gaseous water for constant pressure and temperature. This observation has paved the way to Avogadro's law [60], discovered by the Italian scientist Amedeo Avogadro in 1811, indicating that all sorts of gases with the same volume at the same temperature and pressure contain the same number of particles, allowing the determination of relative atomic masses. This could be achieved by weighing a certain volume of the unknown substance and comparing this mass with a reference, for example hydrogen, stored in the identical volume, yielding the relative mass of the unknown substance.

This measurement procedure has been constantly improved by different researchers, among others by the Swedish chemist Jöns Jacob Berzelius from the Karolinska Institute in Stockholm [61]. The challenge was to achieve very clean samples of chemical substances without any impurities. In 1840 the French chemist Jean-Baptiste Dumas from the University of Paris together with the Belgian chemist Jean Servais Stas measured the masses of oxygen and carbon very precisely by setting oxygen as the reference mass to 16 mass units [62]. From this point the oxygen mass has been used as the reference mass for atomic mass measurements.

Later Stas measured many other masses [63, 64] and has paved the way for the periodic table of elements, invented by the Russian chemist Dmitri Mendeleev [65] and the German chemist Julius Lothar Meyer [66] among others in 1869.

All these efforts culminated in the first mass table, published by the American chemist Frank Wigglesworth Clarke in 1882, where hydrogen is listed with the relative mass of $m(\mathrm{H}) = 1.00\,(1) \times 1/16\,m\,(\mathrm{O})$ [1, 67]. The American chemist Theodore William Richards perfected the determination of atomic masses by accurate chemical stoichiometry and gravimetric measurements. During his PhD project in 1886 he measured the mass of hydrogen with a precision of 2×10^{-3} [9]. From 1887 until 1932 he measured the atomic weights of 55 elements with high precision [68], resulting in the Nobel Prize for Chemistry in 1914. The most precise mass measurement with chemical methods for the hydrogen mass was conducted by the American chemist Edward Williams Morley in Cleveland at the Case Western Reserve University; he reached a precision of 4×10^{-4} in 1895 [12, 13].

In the 19$^{\mathrm{th}}$ century some researchers used the hydrogen mass, and others used the oxygen mass as their reference; it was important to decide for one. In 1903 the International Committee of Atomic Weights officially chose oxygen 16 as reference mass [69, 70]. At this time hydrogen was tabulated with $m\,(\mathrm{H}) = 1.008\,(3) \times 1/16\,m\,(\mathrm{O})$ [67, 71].

At the same time new methods in physics paved the way for the first mass spectrometer. In 1886 the German physicist Eugen Goldstein conducted first experiments with negatively charged cathode rays, which he named canal rays [72, 73]. Later the German physicist Wilhelm Wien showed that these rays could be deflected by magnetic fields [74]. In 1897 the English physicist Joseph John Thomson from the University of Cambridge improved the vacuum of the discharge tube and found negatively charged particles, which were a factor of 2000 lighter compared to the lightest atoms (hydrogen atom) [75]. This was the discovery of the electron, for which he got the Nobel Prize in Physics in 1906.

For further investigations of the positively charged canal rays, he set up an experiment with an electric and a magnetic field, which deflected the ions in different directions [76]. There, he observed special parabolas for every different charge-to-mass ratio of the ion on a photographic plate, which marked the first recorded mass spectrum by a mass spectrograph. These have also been the first phase-sensitive mass measurements with very short evolution times of the ions. Thomson's investigations led to the first observation of isotopes for the element neon (^{20}Ne and ^{22}Ne) in 1913 [77, 78]. Based on these observations the English chemist Frederick Soddy developed the theory of isotopes [79], leading to his Nobel Prize in Chemistry in 1921.

The proton itself was experimentally discovered in 1917 at the University of Manchester by the New Zealand-born British physicist Ernest Rutherford, who published his results in 1919 [80]. He gave the proton its name due to Prout's idea, emphasizing that the proton is the lightest element.

It was possible to deduce the mass of the proton based on the mass of hydrogen and the mass of the electron due to the knowledge of Rutherford's and Bohr's atomic models, proposed earlier in 1911 and 1913 [81, 82].

One of Thomson's research assistants was the English chemist and physicist Francis William Aston. He improved the quality of the ion beam by introducing two slits to achieve a collimated ion beam. Furthermore, he changed the arrangement of the magnetic and electric fields in such a way that the same ions are focused independently of their velocity (velocity-focusing) [83]. In 1920 the hydrogen and helium masses were measured to $m\,(\mathrm{H}) = 1.008\,(1) \times 1/16\,m\,(\mathrm{O})$ and $m(\mathrm{He}) = 4.000\,(1) \times 1/16\,m\,(\mathrm{O})$ [14, 15].

Based on these results the English astronomer Arthur Stanley Eddington could explain the so-called hydrogen burning to be the source of the sun's energy [84]. Aston's measurements with his second apparatus confirmed the observation of the so-called mass defect in 1927 [16]. This is the deviation from the measured masses to the sum of the masses of all protons and neutrons. These measurements laid the experimental foundation for the later discovered nuclear shell structure, found by the German-born American theoretical physicist Maria Goeppert-Mayer in 1948 [85], leading to the Nobel Prize in Physics in 1963.

In Chicago the Canadian-American physicist Arthur Jeffrey Dempster constructed a direction-focused mass spectrometer in 1918 [86]. This was a complementary approach compared to Aston's velocity-focusing. In the 1920s Dempster concentrated his research on medium-heavy atomic masses, for example: potassium, calcium and zinc [87, 88]. On the other hand Aston measured the masses of light atoms, for example hydrogen, deuterium and carbon[2]. Due to his efforts he was awarded the Nobel Prize in Chemistry in 1922.

In 1936 Aston built a third spectrograph and reached a relative precision of 4×10^{-5} for the mass of hydrogen [18]. At this point physical mass determinations were equally precise compared to the chemical ones. However, it turned out that the mass spectrographs have finally proved superior compared to gravimetric stoichiometry.

In the 1930s the precision of mass spectrographs was improved by different groups. The Austrian physicists Josef Mattauch and Richard Herzog were the first who developed the idea of combined velocity and direction-focusing of the ion beam in 1934 [89, 90]. Based on their ideas several "double-focusing" mass spectrographs were built. This is basically the implementation of a special selection technique, namely to only use ions with a certain energy or temperature. Mattauch and Herzog built such a mass spectrograph in Vienna [20], and Dempster [91] set up one in Chicago. Additional mass spectrographs were built by the American physicist Kenneth Tompkins Bainbridge at Harvard University [92] and by the Japanese physicist Koreichi Ogata in Osaka [93]. With these first double-focusing mass spectrographs a relative precision up to 3×10^{-6} was achieved by Mattauch in 1939 [94].

[2] At the same time several so-called sub-standards were established, such as hydrogen, deuterium and carbon. Often hydrogen was measured against deuteron. On the other hand deuteron

After World War II the next generation of mass spectrometers has been built. Higher precision was achieved by larger spectrometers, including second order velocity and direction-focusing. Therefore, these larger spectrometers allow for longer evolution times, resulting in more precise phase measurements. Additionally, the mass lines were recorded electronically instead of using a photographic plate. Leading persons in the field of light masses were besides Bainbridge and Ogata also the American physicist Alfred Otto Carl Nier in Minnesota [95] and the German physicist Heinz Ewald in Mainz [96]. In the group of Nier these efforts culminated in a relative precision of 2×10^{-7} in 1956 [27].

In 1960 the reference for atomic masses (u) was changed to 1/12 of $m(\mathrm{C})$, which influenced the value of the hydrogen mass, but not its precision. The next major improvement was accomplished by the American physicist Lincoln Smith in Brookhaven by the development of a radio-frequency mass spectrometer, the so-called "mass synchrometer" in the late 1950s [97–99]. There the cyclotron frequencies of ions are measured after circulating several times in a magnetic field. Consequently, the evolution time of the ions could be increased drastically. Moreover, the determination of frequencies is superior compared to the determination of spatial distances. This led to a higher precision. In 1971 Smith measured the proton's atomic mass with a relative precision of 5×10^{-9} [39].

Further improvement in precision by two orders of magnitude was achieved by the introduction of the Penning trap by the German-American physicist Hans Georg Dehmelt [100]. Here, the charge-to-mass ratio q/m of a particle stored in an external homogeneous and static magnetic field B is related to its cyclotron frequency:

$$\nu_c = 1/(2\pi) \cdot q/m \cdot B \quad . \tag{1.1}$$

The principal idea is to measure the cyclotron frequency of the ion of interest and compare it with the one of a reference ion (ref), whose mass is known or measured with higher relative precision. Both cyclotron frequencies are measured within the same magnetic field to cancel this. The mass of an ion is then given by:

$$m \;=\; \frac{\nu_c(\mathrm{ref})}{\nu_c} \;\cdot\; \frac{q}{q(\mathrm{ref})} \;\cdot m(\mathrm{ref}) \quad . \tag{1.2}$$

As the charge ratio is assumed to be a ratio of two known integer numbers, the mass ratio can be determined via the measurement of the cyclotron frequency ratio ($\mathcal{R}^{\mathrm{CF}}$). Dehmelt's discovery led to his Nobel Prize in Physics in 1989.

Leading experiments were carried out by Robert Van Dyck Jr. at the University of Washington, who had been an assistant of Dehmelt [42–44]. Two other groups performed atomic mass measurements of the proton, using Penning traps: The group of the American physicist David Pritchard at the Massachusetts Institute

was measured against oxygen or carbon. It was possible to publish a more precise proton mass by the reevaluation of the mass ratio of deuteron against oxygen. Therefore, it is sometimes difficult to quote the correct author for the improved precision of the proton mass, since the proton mass in units of the oxygen's mass is determined by a combination of several links.

of Technology (MIT) [45, 46] and the German-Swedish physicist Reinhold Schuch in Stockholm [48–51]. The literature value of CODATA from 2014 is based on the results of these three groups, yielding a relative precision of 9×10^{-11} [101].

In 2017 we could measure the proton's atomic mass with a relative precision of 3×10^{-11} and with a deviation of more than three sigma to the CODATA 2014 value [52, 53]. The current literature value of CODATA from 2018 for the proton mass has a relative precision of 5.3×10^{-11}, which already includes our result [102]. Today phase evolution times of ions in the order of 10 s or more are possible.

This overview once again reminds us that "If we have seen further it is by standing on the shoulders of giants" [103]. To collect all the information for this overview, the following sources were the most helpful ones: [104], [105], [106] and [107].

1.3 Motivation for the LIONTRAP experiment

The electron, the proton and the neutron are the central building blocks of our visible universe. The precise knowledge of their properties and also the characteristics of their simplest combinations like the atomic nuclei deuteron, triton and helion are of utmost importance for metrology and for tests of fundamental physics. Furthermore, the three isotopes of hydrogen are some of the most precisely measured atomic masses in the periodic table of elements. Together with the mass difference of helion (h,$^3He^{2+}$) and tritium (T) these values constitute a set of important parameters for consistency checks of the SM and for searches of physics beyond the SM, for example via the determination of the electron antineutrino rest mass in the KATRIN experiment (Karlsruhe Tritium Neutrino Experiment) [108].

However, the most precisely measured light ion masses are currently internally inconsistent: The mass of ^{3}He and HD can be independently related to u, see Fig. 1.2. The resulting difference deviates from the directly measured values by five standard deviations, see Table 1.1.

Table 1.1: Inconsistency of light ion masses. The mass difference of $^3He^+$ and HD^+ [109], measured in the group led by Edmund Myers at the Florida State University in Tallahassee (FSU), deviates by five standard deviations from the one calculated based on the atomic masses of proton, deuteron and helion [52, 53, 110]. The values for the atomic masses of deuteron and helion have been measured in the UW-PTMS experiment (University of Washington Penning-Trap Mass Spectrometer) by Van Dyck Jr. at the University of Washington (UW), whereas the proton mass has been measured by the authors' group (MPIK).

$m_p + m_d - m_h\,(10^{-12}\,u)$	Group
5 897 432 675 (67)	MPIK, UW [52, 53, 110]
5 897 432 191 (70)	FSU [109]
484 (97)	Discrepancy

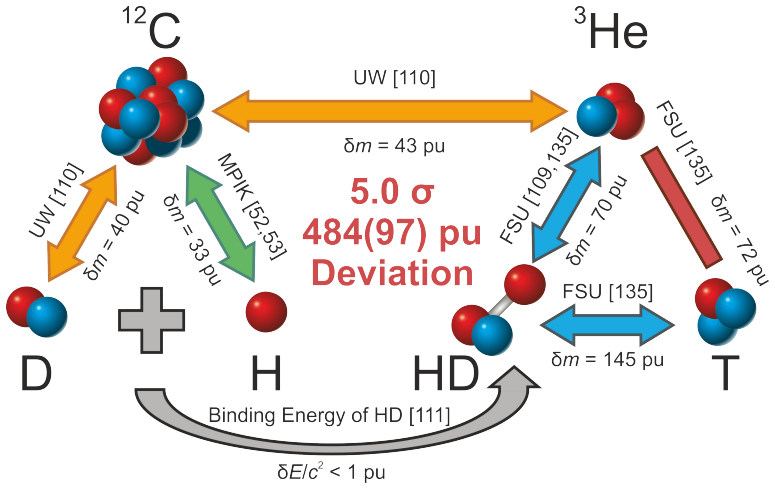

Figure 1.2: The puzzle of light ion masses. The orange and blue links are $\mathcal{R}^{\mathrm{CF}}$s measured at the UW-PTMS and the FSU, respectively. The green link is the proton's atomic mass measured by the LIONTRAP experiment within this work. Here, only the most precise measurements together with their absolute uncertainties in pu (10^{-12} u) are shown for each link. Since the mass of the HD molecule can be calculated from the masses of D and H together with its binding energy [111], this gives an additional link. A $5.0\,\sigma$ discrepancy remains by applying all links, see Table 1.1. Furthermore, the red bar shows the $\mathcal{R}^{\mathrm{CF}}$ requested by KATRIN [112]. The figure is reproduced from [53].

The proton mass

While the proton, in contrast to the electron, is not an elementary particle, its mass m_{p} can still be considered as a fundamental constant. It consists of two up quarks and one down quark, whose individual rest masses contribute to the proton mass by less than 1%. More than 99% of the total mass is stored in their binding energy carried by gluons, which are the exchange particles of the strong nuclear force. Therefore, the quarks move with a velocity close to the speed of light leading to a relativistic mass increase of a factor of roughly one hundred. Furthermore, it is not possible to detect these light quarks directly nor determine their masses. Only the experimentally measured proton mass together with lattice quantum chromodynamics calculations enable the determination of the bare up and down quark masses with a relative precision of $\delta m_{\mathrm{up}}/m_{\mathrm{up}} \approx \delta m_{\mathrm{down}}/m_{\mathrm{down}} \approx 10\%$ [113–115]. The most precise measurement of the proton's atomic mass prior to this work was carried out at the UW-PTMS with a relative uncertainty of $\delta m_{\mathrm{p}}/m_{\mathrm{p}} = 1.4 \times 10^{-10}$ [44].

The dimensionless proton-to-electron mass ratio μ is a crucial parameter in atomic physics. The newly measured proton's atomic mass led to the most precise value for $\mu = m_{\mathrm{p}}/m_{\mathrm{e}}$ with $\delta\mu_{\mathrm{MPIK}}/\mu_{\mathrm{MPIK}} = 4.3 \times 10^{-11}$. μ_{MPIK} is the value which is calculated using the proton and electron masses $m\,(\mathrm{e}^-)$ all determined

in our group [52, 53, 116, 117]. There are additional independent experimental approaches for the measurement of μ, see Fig. 1.3. In one experiment laser spectroscopy of single-photon transitions in antiprotonic helium $\left(\bar{\mathrm{p}}\mathrm{He}^{+}\right)$ at Rydberg states of $n \approx l - 1 \approx 38$ is performed [118]. Here, the antiproton-to-electron mass ratio is measured. In another experiment μ is measured by Doppler-free spectroscopy of the rovibrational level structure of sympathetically cooled HD^{+} molecules [119]. In both approaches the spectroscopy results are combined with theory calculations to extract μ. All experimental values are in excellent agreement with each other. However, they are at least a factor of eighteen less precise compared to μ_{MPIK}. Additionally, various groups study a possible variation of μ over time, which would indicate new physics [120].

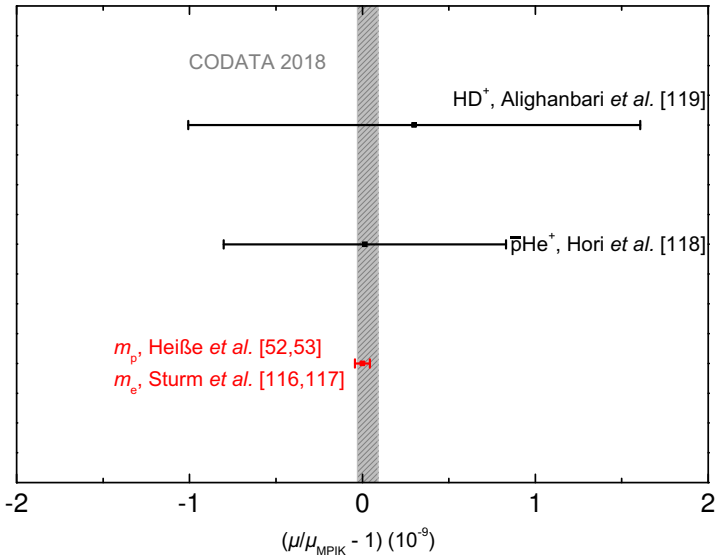

Figure 1.3: Proton-to-electron mass ratios measured with different experimental approaches. For each approach only the most precise value is shown. The gray band represents the CODATA value of 2018 [102]. This value is formed by dividing the CODATA 2018 literature values for the proton's atomic mass and the electron's atomic mass, while the latter is completely dominated by the measurement described in [116, 117].

m_{p} also enters the determination of the Rydberg constant R_{∞} via the reduced mass of the hydrogen atom [101, 121]. The Rydberg constant can be determined by the spectroscopy of the 1S-2S transition frequency of regular hydrogen [122] combined with an independent value of the proton charge radius, resulting in an uncertainty of $\delta R_{\infty}/R_{\infty} = 1.9 \times 10^{-12}$ [102]. If the value for the proton charge radius is only taken from muonic hydrogen spectroscopy, an uncertainty

of $\delta R_\infty / R_\infty = 8 \times 10^{-13}$ is achieved [123], while this measurement is still being discussed in the context of the proton radius puzzle [124, 125]. The value of R_∞ is relatively shifted by 1.6×10^{-13} due to the discrepancy of three standard deviations of m_p (2.8×10^{-10} u) compared to the CODATA 2014 value.

Furthermore, the proton's atomic mass is required for the determination of the hydrogen anion mass, which is used for the most precise comparison of the antiproton-to-proton charge-to-mass ratio [126]. At this experiment, the $(q/m)_{\mathrm{H}^-}$ ratio of the anion H^- is compared to the $(q/m)_{\bar{\mathrm{p}}}$ ratio of the antiproton. Therewith, the electron-to-proton mass ratio, the electron affinity of hydrogen, the electron binding energy and the polarizability shift need to be accounted for. If the invariance under the charge, parity, time-reversal (CPT) transformation holds the precision for the theoretically predicted antiproton-to-proton charge-to-mass ratio has been limited by the uncertainty of the electron-to-proton mass ratio dominated by the proton's atomic mass based on the CODATA 2014 value.

The proton's atomic mass is also essential for the determination of several precisely known atomic masses, for example: ^{13}C, ^{15}N, ^{29}Si, ^{31}P and ^{33}S [127, 128]. It enters their masses since the measured mass doublets involve molecules containing hydrogen.

The deuteron mass

The knowledge of the deuteron mass m_d is essential to determine the neutron mass m_n, since this nucleus consists of a proton and a neutron. It is necessary to measure m_p, m_d and the nuclear binding energy of the deuteron $E_\gamma(\mathrm{d}) \approx -2.4 \times 10^{-3}\,\mathrm{u} \times c^2$ to very high precision to extract m_n via $m_\mathrm{n} = m_\mathrm{d} - m_\mathrm{p} - E_\gamma(\mathrm{d})/c^2$. c denotes the speed of light in vacuum and $E_\gamma(\mathrm{d})$ has been measured with the GAMS4 flat-crystal spectrometer at the Institut Laue-Langevin (ILL) with a relative uncertainty of $\delta E_\gamma(\mathrm{d})/E_\gamma(\mathrm{d}) = 1.8 \times 10^{-7}$ [129, 130]. m_n in combination with m_p is relevant for the determination of nuclear binding energies.

It is furthermore possible to provide a precise test of the equivalence of mass and energy ($E = mc^2$) within special relativity at low energies using the neutron mass [131]. To this end, the mass difference of the mother and daughter nuclei of a neutron capture reaction is measured, for example $^{32}\mathrm{S} + \mathrm{n} \rightarrow {}^{33}\mathrm{S} + \gamma$. The daughter nucleus is produced in an excited state and decays via the emission of gamma photons, whose energy E_γ can be measured with a gamma spectrometer. Consequently, the measured mass difference, the neutron mass and the photon energy have to obey the relation: $(m(^{32}\mathrm{S}) + m_\mathrm{n} - m(^{33}\mathrm{S})) \times c^2 = \Delta m c^2 = E_\gamma(^{33}\mathrm{S})$. Any deviation of this would indicate a violation of $E = mc^2$.

Up to now the most precise test of this relation was carried out by the precise measurement of $m(^{32}\mathrm{S})$, $m(^{33}\mathrm{S})$ together with $E_\gamma(^{33}\mathrm{S})$ as well as $m(^{28}\mathrm{Si})$, $m(^{29}\mathrm{Si})$ and $E_\gamma(^{29}\mathrm{Si})$ [132]. All results combined lead to $(1 - \Delta m c^2/E_\gamma) = -1.4(4.4) \times 10^{-7}$. However, the overall uncertainty is dominated by the statistical uncertainty of $E_\gamma(^{33}\mathrm{S})$ and $E_\gamma(^{29}\mathrm{Si})$, which is hard to overcome using these nuclides due to the small cross sections for the corresponding neutron captures.

The chlorine isotope ^{36}Cl has a significantly larger neutron capture cross section. Up to now the relative uncertainty of $E_\gamma(^{36}\mathrm{Cl})$ is 2.1×10^{-7}, which has been achieved by GAMS4 [133]. It is planned to reach a relative uncertainty of 1×10^{-8} with the GAMS6 spectrometer for $E_\gamma(^{36}\mathrm{Cl})$ and for $E_\gamma(\mathrm{d})$. Combined with an additional mass ratio measurement of the two chlorine isotopes $m(^{35}\mathrm{Cl})$ and $m(^{36}\mathrm{Cl})$ this enables an improved test of special relativity. Here, a relative precision below 2.5×10^{-12} should be achieved to complement the precision expected for $E_\gamma(^{36}\mathrm{Cl})$ measured by GAMS6. This mass ratio is planned to be measured with PENTATRAP, a high-precision mass spectrometer placed at the Max-Planck-Institute for Nuclear Physics in Heidelberg [134, 135]. With these upcoming measurements it would be possible to directly test $(1 - \Delta mc^2/E_\gamma)$ at a level of 2×10^{-8}, which will improve the current best result by more than a factor of 20.

The masses of triton and helion

The aim of the KATRIN experiment is the determination of the electron antineutrino rest mass $m(\bar{\nu}_e)$. For this purpose the beta decay spectrum of tritium is studied. E_0 is the endpoint of the beta decay spectrum if the neutrino mass would be zero, see Fig. 1.4. The mass difference of the triton m_t and helion m_h is related to this endpoint via $(m_\mathrm{t} - m_\mathrm{h} - m(\mathrm{e}^-))\,c^2 = E_0 = E_\mathrm{max} + m(\bar{\nu}_e)\,c^2$, where E_max is the measured endpoint of the beta decay spectrum. The knowledge of this mass difference is essential to reach highest sensitivity of the electron antineutrino rest mass [112]. The final aim for the sensitivity of KATRIN is a 90% confidence of $m(\bar{\nu}_e) \leq 0.2\,\mathrm{eV/c^2}$, if the neutrino mass is unmeasurably small, and a more than five sigma significance if $m(\bar{\nu}_e) > 0.35\,\mathrm{eV/c^2}$ [108]. For a central consistency check the $\mathcal{R}^\mathrm{CF}$ of triton and helion is requested. Today this $\mathcal{R}^\mathrm{CF}$ is known with a relative uncertainty of 2×10^{-11} [136].

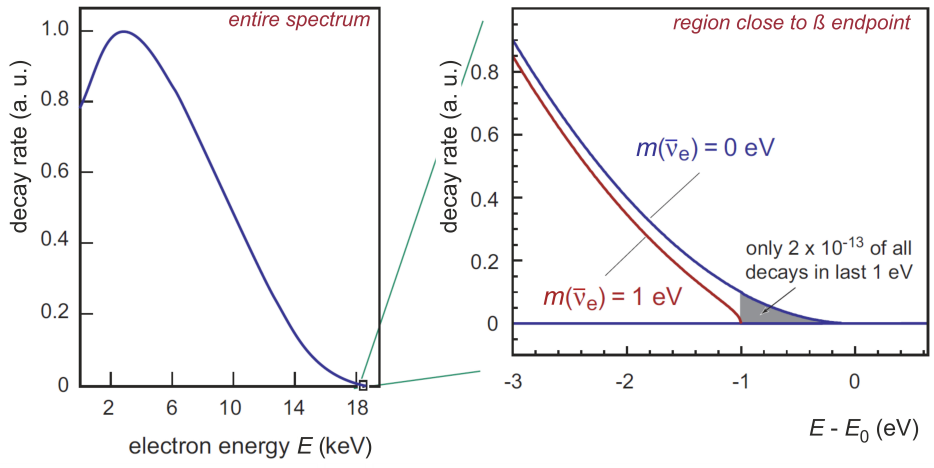

Figure 1.4: Entire beta decay spectrum of tritium (left) and at the endpoint region (right). E_0 is the endpoint energy for zero neutrino mass. The figure is reproduced from [137].

2 Measurement fundamentals

2.1 Penning-trap basics

Frequencies are the quantities which can be measured with highest precision in physics. To determine the cyclotron frequency of a charged particle very precisely a long measurement time is favorable. One possible experimental tool is to make use of a magnet to confine the particle in radial direction, the x-y-plane, by the Lorentz force. For a static magnetic field the cyclotron motion of a charged particle confines it merely to the perpendicular plane ($x - y$ plane) of the magnetic field lines, but not in the parallel direction z. Due to Earnshaw's theorem it is not possible to store a charged particle in a stable stationary equilibrium neither by a single static magnetic field nor by a single static electric field [138]. The trapping of particles is possible by either a time-varying electric or magnetic field or by a combination of a static magnetic and a static electric field. For a high-precision measurement of the cyclotron frequency the latter is favorable, since the magnetic field generated by a superconducting magnet is typically more stable compared to the time-varying electric field.

An additional electrostatic quadrupole potential can be applied to confine the particle along the magnetic field axis. Such a superposition of a static magnetic field and a static electric field is realized in a so-called Penning trap. To measure the cyclotron frequency of a particle non-destructively and with highest precision, such a Penning trap is the experimental tool of choice. Two different Penning-trap designs are commonly used in experiments to generate the electric quadrupole potential: hyperbolically shaped trapping electrodes [100] and the cylindrically shaped trapping electrodes [139], see Fig. 2.1. In their simplest form both types consist of three electrodes, the inner one is on the potential U_R, whereas the two outer ones (endcaps) are at ground potential. The electric potential V around the trap center can be expressed in cylindrical coordinates ρ, z by:

$$V(\rho, z) = \frac{U_\mathrm{R}}{2} \sum_{n=0,2,4}^{\infty} \frac{C_n}{d_\mathrm{char}^n} \sum_{k=0}^{\frac{n}{2}} \frac{(-1)^k \, n!}{2^{2k} \, (n-2k)! \, (k!)^2} z^{n-2k} \rho^{2k} \quad , \tag{2.1}$$

where $d_\mathrm{char} = 1/2 \cdot \sqrt{2 \cdot dz_0^2 + r_0^2}$ is the characteristic trap size, defined by the radius of the trap electrodes r_0 and the axial distance of the endcaps to the trap center dz_0. To achieve an ideal trapping potential, all coefficients C_n with $n \geq 4$ should be zero.

The motion of the stored particle in such a superposition of an electric quadrupole and static magnetic field can be decomposed into three eigenmotions: two radial

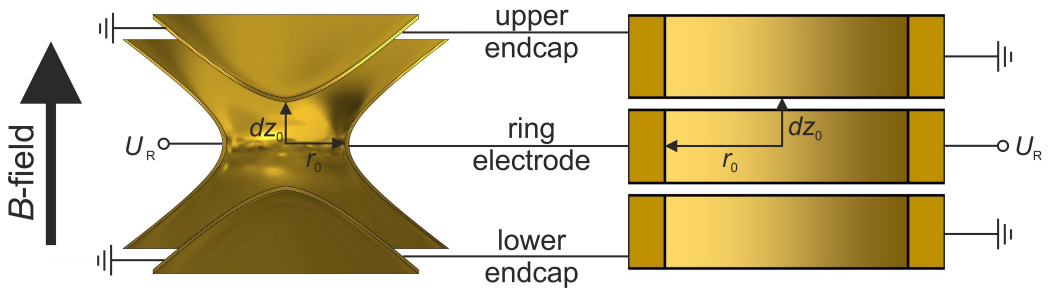

Figure 2.1: Comparison of a hyperbolically shaped Penning trap (left) [100] and a cylindrically shaped one (right) [139]. The top and bottom electrodes (endcaps) are at ground potential, whereas the ring voltage U_R is negative for positively charged particles. For suitable values of B and U_R the particle is confined with the generated quadrupole potential in the axial direction, whereas the magnetic field ensures the confinement in radial direction. Furthermore, the two characteristic trap dimensions r_0 and dz_0 are shown. For details see text.

motions with the corresponding frequencies ν_+, ν_- and one axial motion with the frequency ν_z. The radial frequencies are denoted as the modified cyclotron frequency ν_+ and the magnetron frequency ν_-, see Fig. 2.2. The three frequencies of the particle are given by:

$$\nu_z = \frac{1}{2\pi}\sqrt{\frac{q}{m}\frac{U_\mathrm{R}C_2}{d^2_\mathrm{char}}} \quad , \tag{2.2}$$

$$\nu_+ = \frac{1}{2}\left(\nu_c + \sqrt{\nu_c^2 - 2\nu_z^2}\right) \quad , \tag{2.3}$$

$$\nu_- = \frac{1}{2}\left(\nu_c - \sqrt{\nu_c^2 - 2\nu_z^2}\right) \quad . \tag{2.4}$$

In our experimental setup the following conditions apply: $B \approx 3.8\,\mathrm{T}$ and $U_\mathrm{R} \approx -10\,\mathrm{V}$. The associated frequencies for a stored proton and carbon ion are listed in Table 2.1.

Table 2.1: Typical eigenfrequencies of a proton and a carbon ion $^{12}\mathrm{C}^{6+}$ in the precicion trap of the LIONTRAP experiment.

	Proton	$^{12}\mathrm{C}^{6+}$
ν_+ (Hz)	57 379 350	28 903 993
ν_z (Hz)	739 873	525 141
ν_- (Hz)	4 771.0	4 771.4
ν_c (Hz)	57 384 120	28 908 764

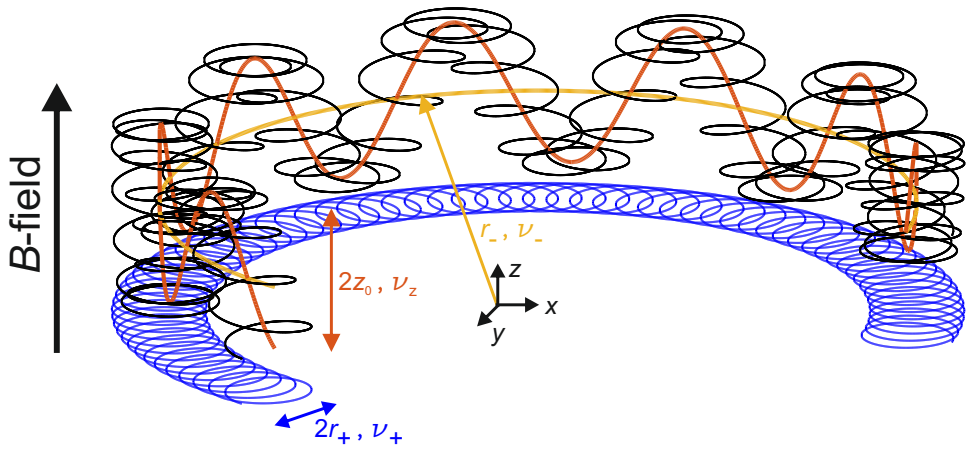

Figure 2.2: Trajectory of a stored particle (black). The motion can be decomposed into three eigenmotions: the modified cyclotron motion with the frequency ν_+ and radius r_+ (blue), the magnetron motion (ν_-, r_-, yellow) and the axial motion with the amplitude z_0 and frequency ν_z (orange).

The energies (E_z, E_+, E_-) and the axial amplitude z_0 as well as the two radii r_+ and r_- of the two radial eigenmotions are related by [140]:

$$E_z = \frac{1}{2} m \left(2\pi\nu_z\right)^2 z_0^2 = k_\mathrm{B} T_z \quad , \tag{2.5}$$

$$E_+ \approx \frac{1}{2} m \left(2\pi\nu_+\right)^2 r_+^2 = k_\mathrm{B} T_+ \quad , \tag{2.6}$$

$$E_- \approx -\frac{1}{4} m \left(2\pi\nu_z\right)^2 r_-^2 = k_\mathrm{B} T_- \quad , \tag{2.7}$$

where k_B is the Boltzmann constant. The total energy of the modified cyclotron frequency is mainly kinetic, whereas the negative potential energy dominates the total magnetron energy. Therefore, the magnetron energy and temperature are negative.

The sought after free cyclotron frequency can be determined via the invariance theorem [141]:

$$\nu_c = \sqrt{\nu_+^2 + \nu_z^2 + \nu_-^2} \quad . \tag{2.8}$$

This formula is immune against a tilt between the magnetic field and the electrostatic quadrupole potential as well as an elliptic deformation of the electrostatic quadrupole potential.

In our experiment we compare the cyclotron frequencies of the proton with the bare carbon ion as a magnetic field sensor. The carbon nucleus has a stronger electronic signal on our detection device and a cyclotron frequency closer to the proton's cyclotron frequency compared to the singly charged carbon ion.

Based on Eq. 1.1 the atomic mass of the proton m_p can be expressed by:

$$m_\mathrm{p} = \frac{1}{6}\frac{\nu_c\left(^{12}\mathrm{C}^{6+}\right)}{\nu_c\left(\mathrm{p}\right)} m\left(^{12}\mathrm{C}^{6+}\right) \quad . \tag{2.9}$$

Here the mass of the bare carbon nucleus is given by:

$$m\left(^{12}\mathrm{C}^{6+}\right) = m\left(^{12}\mathrm{C}\right) - 6m_\mathrm{e} + \textstyle\sum_{i=1}^{6} \frac{E_{b,i}}{c^2} \tag{2.10}$$

$$= 11.996\,709\,626\,413\,85\,(8)\,\mathrm{u} \quad , \tag{2.11}$$

were $E_{b,i}$ are the binding energies of the six removed electrons [142]. The mass of the carbon ion $^{12}\mathrm{C}^{6+}$ can be determined with a relative precision of 0.08 ppt. This uncertainty arises due to the current uncertainty of the binding energies and the masses of the six removed electrons.

Thus, the goal is to measure both cyclotron frequencies in the same magnetic field very precisely. The cyclotron frequency is mainly given by ν_+ due to the strong hierarchy of the three eigenfrequencies ($\nu_+ > \nu_z > \nu_-$) for our experimental conditions. Therewith, the uncertainty of ν_c is dominated by the uncertainty of ν_+, which again strongly depends on the magnetic field stability.

2.2 Cyclotron frequency ratio ($\mathcal{R}^{\mathrm{CF}}$) measurement

For an ideal $\mathcal{R}^{\mathrm{CF}}$ measurement the cyclotron frequencies of both ions are measured at the same time to exclude temporal magnetic field fluctuations or drifts, at the same place to guarantee the identical magnetic field and with small energies to avoid large systematic shifts. A particular challenge when comparing a proton to a carbon ion arises from the large q/m difference of these ions. In Penning traps doublets with similar q/m ratios are favorable. Consequently such doublets then have similar cyclotron frequencies and similar frequency shifts; most systematic frequency shifts in the $\mathcal{R}^{\mathrm{CF}}$ cancel to a large extent.

For stable light nuclei relative mass uncertainties in the order of 10^{-11} are reached nowadays. These masses are given in atomic mass units (u) with the definition: $1\,\mathrm{u} = \frac{1}{12} m\left(^{12}\mathrm{C}\right)$. The most precise directly measured atomic masses of light particles are summarized in Table 2.2. Among these, the atomic mass of $^{16}\mathrm{O}$ is the one known best with a relative uncertainty of 11×10^{-12} [143, 144]. This measurement took place in a group led by Robert Van Dyck Jr. at the UW-PTMS experiment (University of Washington Penning-Trap Mass Spectrometer). The most precise atomic mass comparison up to now was done in the group of David Pritchard at the Massachusetts Institute of Technology. Using a specialized technique, his group was able to compare $m\left(^{14}\mathrm{N}_2^+\right)$ and $m\left(^{13}\mathrm{C}_2\mathrm{H}_2^+\right)$, a close-to-perfect mass doublet, with a relative precision of 7×10^{-12} [145]. Further precise mass ratios are listed in Table 2.3.

Table 2.2: Overview of the most precise directly measured atomic masses and their uncertainties. All values in the table correspond to the individual mass measurement of this particle with the lowest uncertainty. The majority of the values have been measured in the UW-PTMS experiment (University of Washington Penning-Trap Mass Spectrometer) by Van Dyck Jr. at the University of Washington (UW), whereas the others have been measured by the authors' group (MPIK). The table is reproduced from [53].

Particle	Atomic masses (u)	$\delta m/m(10^{-12})$	Group
e^-	0.000 548 579 909 069 (15)	28	MPIK [116, 117][1]
p^+	1.007 276 466 598 (33)	33	MPIK [52, 53]
d^+	2.013 553 212 745 (40)	20	UW [110]
^{3}He	3.016 029 321 675 (43)	14	UW [110]
^{4}He	4.002 603 254 131 (62)	15	UW [144, 146]
^{16}O	15.994 914 619 57(18)	11	UW [143, 144]

There are two different approaches described in the literature so far to reduce the uncertainty originating from the magnetic field stability. For particularly well-suited ion pairs, with q/m ratios which differ by less than 0.06 %, simultaneous $\mathcal{R}^{\mathrm{CF}}$ measurements have been performed in the Pritchard group using coupled magnetron motions of two ions in the same trap, the so-called "Ion balance" [132, 145]. The very similar q/m ratios of the ion pair ensures efficient magnetron coupling at ion distances large enough to not cause significant frequency shifts from the Coulomb repulsion between them. The magnetic field jitter cancels to a large extent. During their measurements they were able to reach relative statistic uncertainties of 3×10^{-12}. Including also the systematic uncertainties the total relative uncertainty amounts to 7×10^{-12}. Up to now these are the most precise cyclotron frequency comparisons.

The second approach relies on a consecutive measurement of the two modified cyclotron frequencies. There, the statistical uncertainty is mainly given by the temporal stability of the magnetic field. A short time span between the modified cyclotron frequency measurements helps to reduce this uncertainty.

In an earlier measurement campaign, the Pritchard group also measured the proton mass using a different technique [45, 46]. They performed a measurement of $m\left(\mathrm{CH}_4^+\right)$ against $m\left(\mathrm{C}^+\right)$ to overcome the large q/m mismatch of the proton and the carbon ion and reduce systematic shifts. The cyclotron frequency of one ion was measured four times and subsequently a new ion of the other type was produced and the measurement was repeated. For the determination of the $\mathcal{R}^{\mathrm{CF}}$ the average magnetic field drift is removed from the measured cyclotron frequencies

[1] The atomic mass of the electron is determined by combining a high-precision measurement of the Larmor-to-cyclotron frequency ratio of $^{12}\mathrm{C}^{5+}$ with state-of-the-art bound state quantum electrodynamics calculations of its g-factor. The experiment has been carried out at the University of Mainz with the predecessor experiment of LIONTRAP.

Table 2.3: Cyclotron frequency ratios measured with relative uncertainties below 50×10^{-12}. Some of them were measured in the group of David Pritchard at Massachusetts Institute of Technology (MIT) with the MIT Penning-Trap Mass Spectrometer. Later experiments with this setup were continued in the group led by Edmund Myers at the Florida State University in Tallahassee (FSU) [147]. The current best antimatter-to-matter charge-to-mass comparison has been carried out by the group led by Stefan Ulmer within the Baryon Antibaryon Symmetry Experiment collaboration (BASE).

Ion pair	$\delta m/m\,(10^{-12})$	Group
$^{3}\mathrm{He}^{+}$ / HD^{+}	23	FSU [109]
T^{+} / HD^{+}	48	FSU [136]
$^{12}\mathrm{C_2H_4^{+}}$ / $^{28}\mathrm{Si}^{+}$	28	FSU [148]
$^{13}\mathrm{C_2H_4^{+}}$ / $^{28}\mathrm{Si}^{+}$	25	FSU [148]
$^{14}\mathrm{N_2^{+}}$ / $^{13}\mathrm{C_2H_2^{+}}$	7	MIT [145]
$^{12}\mathrm{CD_3^{+}}$ / $^{18}\mathrm{O}^{+}$	50	FSU [149]
$^{13}\mathrm{CD_3^{+}}$ / $^{19}\mathrm{F}^{+}$	48	FSU [149]
$^{16}\mathrm{O_2^{+}}$ / $^{31}\mathrm{PH}^{+}$	27	FSU [148]
$^{28}\mathrm{SiH_3^{+}}$ / $^{31}\mathrm{P}^{+}$	29	FSU [148]
$^{28}\mathrm{SiD_3^{+}}$ / $^{17}\mathrm{O_2^{+}}$	38	FSU [150]
$^{29}\mathrm{Si}^{+}$ / $^{28}\mathrm{SiH}^{+}$	7	MIT [132]
$^{33}\mathrm{S}^{+}$ / $^{32}\mathrm{SH}^{+}$	9	MIT [132]
$^{86}\mathrm{Kr}^{2+}$ / $^{84}\mathrm{Kr}^{2+}$	48	FSU [151]
H^{-} / $\bar{\mathrm{p}}$	69	BASE [126]

by interpolating between the different measurement points. The magnetic field fluctuations were the dominant uncertainty in their measurements.

At the UW-PTMS experiment the cyclotron frequency of a single proton was measured for several hundred times, before the reference carbon ion C^{4+} was created and $\nu_c\left(\mathrm{C}^{4+}\right)$ was non-destructively measured for several hundred times, too. Additionally, the ring voltage was changed by a factor of around two to measure the axial frequencies of both ions with the same detector. After these measurements the scheme is repeated. Finally, the magnetic field drift is corrected for from the measured cyclotron frequencies. These long time spans during the $\mathcal{R}^{\mathrm{CF}}$ determination were less critical due to the stable magnetic field of $1/B \times \delta B/\delta t \approx 17(2)\,\mathrm{ppt/h}$ during the proton mass measurement [44]. Later the stability was improved even more to $1/B \times \delta B/\delta t \approx 0.1\,\mathrm{ppt/h}$ [152].

In the group led by Edmund Myers the $\mathcal{R}^{\mathrm{CF}}$ is determined in two successive measurements. There, one ion is excited to a large modified cyclotron radius of around 2 mm, while measuring the cyclotron frequency of the other ion in the trap center twice. The scheme is repeated several times.

The magnetic field drift is removed from the measured cyclotron frequencies by interpolation, too. With this method the new creation of the ions is avoided and the switching between the two measured ions is realized within about 4 min [109].

However, since the proton and the carbon ion are no charge-to-mass doublet it is not possible to use the "Ion balance method". At LIONTRAP we therefore make use of the second approach, a successive measurement of the two modified cyclotron frequencies within a short time span, see Fig. 2.3. Compared to previous setups, the LIONTRAP precision trap has four different precisely tuned detection systems. Thus, it is possible to measure the axial frequency and the cyclotron frequency of the proton and the carbon ion at the same electrical trapping potential. With this method the switching time is shorter than one minute, while an interaction between the two ions is strongly suppressed. Additionally, this approach reduces the impact of the magnetic field fluctuations dramatically in comparison to a new creation and preparation of single ions. This configuration furthermore allowed several systematic studies of the new precision trap. Further information are provided in section 3 and 4 of the second paper, see chapter 3.2.

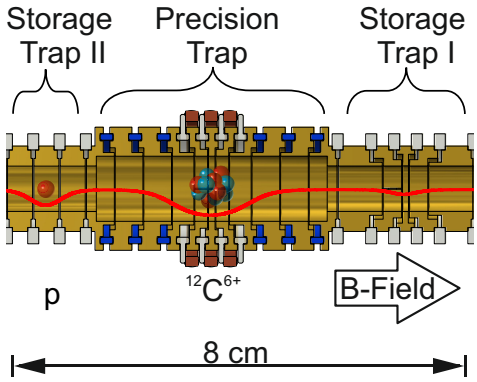

Figure 2.3: Sectional view of the trap tower including the two separate storage traps (ST-I, ST-II) and the precision trap (PT). By shuttling the ions between the storage traps and the PT, the time between successive modified cyclotron frequency measurements is minimized. Furthermore the identical electrical field configurations (red line) for both ions guarantee the identical position of the ions in the PT and therewith the same magnetic field for the $\mathcal{R}^{\mathrm{CF}}$ measurement.

2.3 Image charge shift

The total uncertainty of a measurement is the combined statistical and systematic uncertainty. The obtained statistical result is corrected for systematic shifts. These can be grouped into energy dependent and energy independent shifts. Since it is possible to vary the energy of the ions during the measurement it is possible to reduce the uncertainty of the corresponding energy dependent shifts.

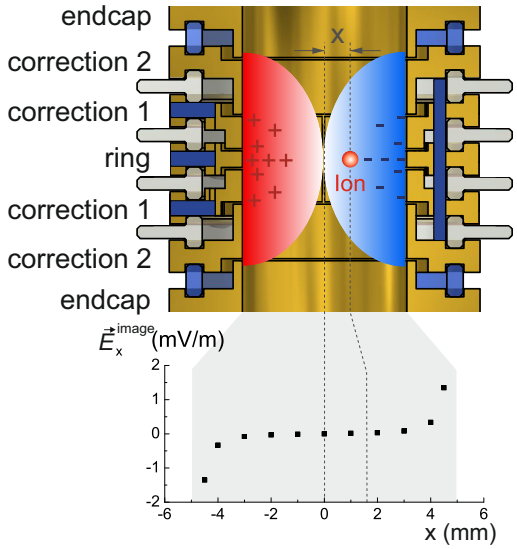

Figure 2.4: Schematic view on the precision trap of the LIONTRAP experiment including the two pairs of correction electrodes for shaping a highly harmonic electrostatic trapping potential. Here, the image charge densities at the surfaces of the electrodes are sketched. Furthermore, the resulting electric field $\vec{E}_{\text{image}}$ is shown. The figure is reproduced from [153].

The image charge shift is the largest energy independent shift for all atomic mass measurements of light ions in our experiment. Thus it was important to experimentally measure this shift with a precision of 5% in another measurement campaign.

Since the ion is a charged particle it induces image charges on the conducting surfaces of the trap electrodes. The generated electric field $\vec{E}_{\text{image}}$ of these charges acts back on the ion's motion and shifts its eigenfrequencies, see Fig. 2.3. This image charge effect can be treated as a perturbation by an additional force $\vec{F} = \vec{E}_{\text{image}} \cdot q$ within the equations of motion. The image charge shift has been precisely determined by simulations in COMSOL, see chapter 3.3.

The precision trap of the LIONTRAP experiment can be approximated with an infinite cylinder were the frequency shifts of the two radial modes can be calculated analytically to:

$$\Delta\nu_{\pm} = \mp\frac{q^2}{16\pi^2\epsilon_0 m r_0^3 \nu_c} \quad , \tag{2.12}$$

where r_0 is the inner trap radius and ϵ_0 is the electrical permittivity. For the infinite cylinder the axial frequency ν_z is not shifted. Furthermore, the cyclotron frequency determined via $\nu_c = \nu_+ + \nu_-$ is unperturbed. The relative shift of the cyclotron frequency determined via the invariance theorem is:

$$\frac{\Delta\nu_c}{\nu_c} = \frac{\nu_c - \nu_c\,(\text{meas})}{\nu_c} \approx \frac{m}{4\pi\epsilon_0 B_0^2 r_0^3} \quad . \tag{2.13}$$

Consequently the image charge shift is especially large for the proton mass measurement since the proton and the carbon ion are no mass and charge doublet. The magnetic field strength of our superconducting magnet is fixed to 3.8 T. Therefore, only the trap radius can be enlarged to reduce this shift. However, this is a trade-off with the electronic signal strength, which is especially small for the singly charged proton and gets smaller with an increased trap radius. Therefore, we decided to enlarge the inner trap radius from 3.5 mm to $r_0 = 5\,\mathrm{mm}$, which reduces this shift by a factor of 3. For the carbon ion in our precision trap the image charge shift amounts to:

$$\left.\frac{\Delta\nu_c}{\nu_c}\right|_{^{12}\mathrm{C}^{6+}} = 99 \cdot 10^{-12} \quad . \tag{2.14}$$

The shift of the $\mathcal{R}^{\mathrm{CF}}$ is given with -91.0×10^{-12}. Since this shift is fixed after manufacturing the trap electrodes, the only way to reduce its uncertainty is to measure this shift very precisely. Therefore, we want to measure this experimentally on a relative 5% level. For this two approaches are possible. Previously this shift has been measured by increasing the number of identical ions in one trap and measuring precisely their cyclotron frequency if the common motion of these ions stays coherent [154]. Since the image charge shift scales linearly with the number of ions it is possible to determine it via the measured slope. With this method it has been possible to determine the shift with a relative precision of 4% [144].

To avoid multi-ion-ion interaction, we decided for a different approach: we directly compare the image charge shift of the proton and the carbon ion. Since the axial frequency is basically unperturbed in the cylindrically symmetric trap, only a comparison of the modified cyclotron frequencies or the magnetron frequencies is reasonable. In our approach we compare the magnetron frequency difference of the carbon ion and the proton, since the absolute shift for the cyclotron and magnetron frequencies is identical and consequently the relative shift of the magnetron frequency is a factor of $\nu_+/\nu_- \approx 6 \times 10^4$ higher compared to the relative shift of the modified cyclotron frequency. Additionally, it is up to now also not possible to determine the modified cyclotron frequency with the required relative precision of 5×10^{-12}.

On the other hand the typical precision of the magnetron frequency measurement is 50 mHz. Such a precision is absolutely sufficient for the determination of the free cyclotron frequency, for example during the proton mass campaign. But to measure the effect of the image charge shift on the magnetron frequency difference a precision of 120 μHz is necessary. To achieve this, a 1000-fold improvement is required. Therefore, we applied a dedicated Ramsey-like measurement scheme described in chapter 3.3. To this end it has been possible to measure the image charge shift directly with a relative precision of 5%, the second most precise measurement on this effect described in the literature. Furthermore, this shift has been measured for the first time in a cylindrical Penning trap.

Since the image charge can also be simulated, we furthermore are able to compare the experimentally measured result with the simulated one. The simulation

is based on finite element methods carried out by my colleague Marc Schuh using the software COMSOL [155]. Here the generated image charge field of a charged particle in our precision trap has been numerically calculated.

The simulation on the image charge effect reaches a relative uncertainty of 1%. All the manufactured electrodes of the LIONTRAP experiment have a total geometry uncertainty of $\pm 20\,\mu$m. This includes the production uncertainty, as well as the uncertainty arising from the alignment of the trap tower and the cooling down of the whole system. This uncertainty is responsible for the largest uncertainty contribution of the simulated results.

The experimental results and simulation agree on the 5% level.

3 Publications

This thesis is written in a cumulative format in agreement with the regulations of the Department of Physics and Astronomy of Heidelberg University. Therefore, it contains a total of three papers, which have been published in or submitted to internationally recognized peer-reviewed *Physical Review Journals*.

The LIONTRAP experiment has been set up during the course of this thesis. This newly developed experimental apparatus allows a variety of measurements. All experimental data of the three papers here presented have been measured with LIONTRAP. The author's contributions to the individual articles are shortly described for each paper.

In section 3.1 the Physical Review Letter about the newly measured atomic mass of the proton and oxygen, which was published in July 2017, is presented. There, the experimental setup and the measurement principle are briefly described. Furthermore, the important concepts of the new experiment are presented. Additionally, an overview of the major systematic uncertainties of the proton mass measurement is given.

In the following section 3.2 the comprehensive paper for the new mass spectrometer LIONTRAP including a detailed evaluation of the proton and oxygen mass is presented. This paper includes an overview about the light ion masses and a brief review of Penning trap physics. Furthermore, the technical details of our detection techniques, detection systems as well as the ion creation are presented. Additionally, the characterization of our new measurement trap, such as the highly harmonic electrostatic quadrupole potential and the measurement of the magnetic field, are presented.

The paper about the theoretical and experimental investigation of the largest systematic shift in the proton mass campaign, the image charge shift, is presented in section 3.3. There, the newly developed measurement concept of the magnetron frequency is presented, allowing a 1000-fold improved precision. Furthermore, a comparison of different simulation approaches for different Penning traps is given. Additionally, the details of the finite element simulation of the image charge shift are provided, including an elaborated determination of its numerical uncertainty.

3.1 High-precision measurement of the proton's atomic mass

In this article the measurement of the proton's atomic mass is described. This article has been published in *Physical Review Letters* and has been chosen as *Editors' Suggestion* article.

Authors: Fabian Heiße, Florian Köhler-Langes, Sascha Rau, Jiamin Hou, Sven Junck, Anke Kracke, Andreas Mooser, Wolfgang Quint, Stefan Ulmer, Günter Werth, Klaus Blaum and Sven Sturm.

Publication status (7/2019): Published.

Journal reference: Phys. Rev. Lett. 119, 033001, (2017).

DOI: 10.1103/PhysRevLett.119.033001 .

Authors' contributions: FH, FKL, SR, WQ, KB and ST planned the experiment. FH, FKL, SR and ST conducted the experiment and took the data. FH, FKL, SR and ST analyzed the data. FH and FKL conducted the final analysis. All authors together discussed the results. FH wrote the manuscript. All authors took part in the critical review of the manuscript before and after submission.

Abstract: We report on the precise measurement of the atomic mass of a single proton with a purpose-built Penning-trap system. With a precision of 32 parts per trillion our result not only improves on the current CODATA literature value by a factor of three, but also disagrees with it at a level of about three standard deviations.

3.2 High-precision mass spectrometer for light ions

In this article the high-precision mass spectrometer for light ions LIONTRAP is described in detail. This article has been accepted in *Physical Review A*.

Authors: Fabian Heiße, Sascha Rau, Florian Köhler-Langes, Wolfgang Quint, Günter Werth, Sven Sturm and Klaus Blaum.

Publication status (7/2019): In press, corrected proof.

Journal reference: Phys. Rev. A 100, 022518 (2019).

DOI: 10.1103/PhysRevA.100.022518 .

Authors' contributions: FH, FKL, SR, WQ, ST and KB planned the experiment. FH, FKL, SR and ST conducted the experiment and took the data. FH, FKL, SR and ST analyzed the data. FH conducted the final analysis. All authors together discussed the results. FH wrote the manuscript. All authors took part in the critical review of the manuscript before and after submission.

Abstract: The precise knowledge of the atomic masses of light atomic nuclei, e.g., the proton, deuteron, triton, and helion, is of great importance for several fundamental tests in physics. However, the latest high-precision measurements of these masses carried out at different mass spectrometers indicate an inconsistency of five standard deviations. To determine the masses of the lightest ions with a relative precision of a few parts per trillion and investigate this mass problem, a cryogenic multi-Penning-trap setup, LIONTRAP (Light-Ion Trap), was constructed. This allows an independent and more precise determination of the relevant atomic masses by measuring the cyclotron frequency of single trapped ions in comparison to that of a single carbon ion. In this paper the measurement concept and a doubly compensated cylindrical electrode Penning trap are presented. Moreover, the analysis of the first measurement campaigns of the proton's and oxygen's atomic mass is described in detail, resulting in $m_\mathrm{p} = 1.007\,276\,466\,598\,(33)\,\mathrm{u}$ and $m(^{16}\mathrm{O}) = 15.994\,914\,619\,37\,(87)\,\mathrm{u}$. The results on these data sets have already been presented by F. Heiße et al. [Phys. Rev. Lett. 119, 033001 (2017)]. For the proton's atomic mass, the uncertainty was improved by a factor of three compared to the 2014 CODATA value.

3.3 Image charge shift in high-precision Penning traps

In this article the experimental measurement of the image charge shift in high-precision Penning traps is described. Furthermore the result is compared with state-of-the-art simulations. This article has been accepted in *Physical Review A*.

Authors: Marc Schuh*, Fabian Heiße*, Tomi Eronen, Jochen Ketter, Florian Köhler-Langes, Sascha Rau, Tom Segal, Wolfgang Quint, Sven Sturm and Klaus Blaum.

*Both authors share the first authorship.

Publication status (7/2019): In press, corrected proof.

Journal reference: Phys. Rev. A 100, 023411 (2019).

DOI: 10.1103/PhysRevA.100.023411 .

Authors' contributions: FH, FKL, SR, WQ, ST and KB planned the experiment. FH, FKL, SR and ST conducted the experiment and took the data. MS, TE, JK and TS conducted and evaluated the simulations. FH, FKL, SR and ST analyzed the data. FH conducted the final analysis. All authors together discussed the results. MS wrote the theory and simulations part of the manuscript. FH and FKL wrote the experimental part of the manuscript. All authors took part in the critical review of the manuscript before and after submission.

Abstract: An ion in a Penning trap induces image charges on the surfaces of the trap electrodes. These induced image charges are used to detect the ion's motional frequencies, but they also create an additional electric field, which shifts the free-space cyclotron frequency typically at a relative level of several 10^{-11}. In various high-precision Penning-trap experiments, systematics and their uncertainties are dominated by this so-called image charge shift (ICS). The ICS is investigated in this work by a finite-element simulation and by a dedicated measurement technique. Theoretical and experimental results are in excellent agreement. The measurement is using singly stored ions alternately measured in the same Penning trap. For the determination of the ion's magnetron frequency with relative precision of better than 10 parts per billion, a Ramsey-like technique has been developed. In addition, numerical calculations are carried out for other Penning traps and agree with older ICS measurements.

4 Discussion

The new Penning-trap setup LIONTRAP has been built and characterized in detail. Its precision trap is the first doubly compensated seven-electrode Penning trap, which gives rise to a very harmonic trapping potential. This allows large enough axial amplitudes to perform the first successful phase-sensitive measurements of the proton's modified cyclotron frequency, see section 3 of the second paper in chapter 3.2.

This again paved the way for the first successful measurement campaign, which results in the most precise determination of the proton's atomic mass, see chapter 3.1 and 3.2. Statistically we could achieve a relative uncertainty of 1.8×10^{-10} after one measurement cycle with a duration of 45 min. Accordingly, within three hours of measurement time we were statistically on the same level as the literature value of CODATA from 2014. We finally ended up with a relative statistical uncertainty of 1.6×10^{-11}, limited by magnetic field fluctuations. The total systematic uncertainty amounts to 2.9×10^{-11}, which is mainly given by the uncertainties of the quadratic magnetic field inhomogeneity, special relativity and the image charge effect, see Table 4.1.

The following discussion will concentrate on these in total four effects, which limit the precision of our proton mass measurement. These limitations are explained in detail and possibilities to reduce and circumvent them in the future are presented.

Table 4.1: Overview of the leading uncertainties of the cyclotron frequency ratio corrected for systematic shifts ($\mathcal{R}_{\mathrm{cor}}^{\mathrm{CF}}$) of the proton mass measurement.

Effect	$\left(\mathcal{R}_{\mathrm{stat}}^{\mathrm{CF}} - \mathcal{R}_{\mathrm{cor}}^{\mathrm{CF}}\right)/\mathcal{R}_{\mathrm{stat}}^{\mathrm{CF}}$ (10^{-12})	Uncertainty (10^{-12})	Improvement factor
Statistical uncertainty[1]		16	2
Residual magnetic inhomogeneity	-20.9	27.4	100
Special relativity	-8.9	7.1	2
Image charge effect	-91.0	4.6	2

[1] This represents the total statistical uncertainty for the proton mass.

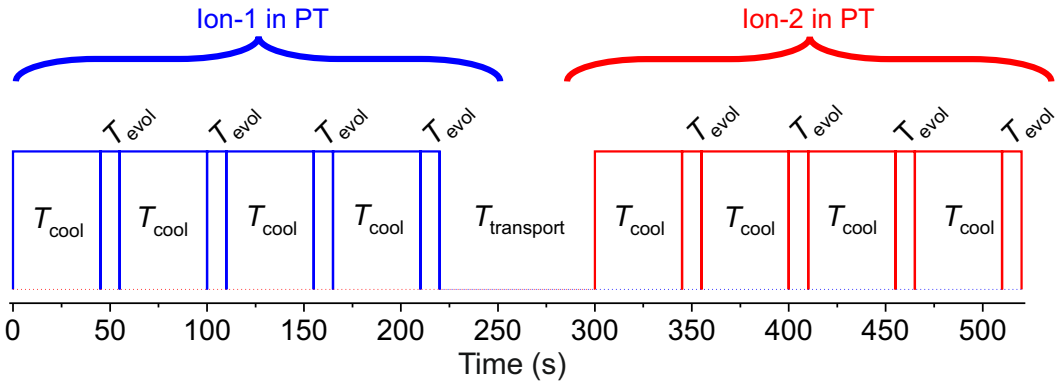

Figure 4.1: Time scheme of the cycle for the measurement of the proton mass, only showing the four PnA cycles to determine the modified cyclotron frequency with highest precision for both ions. The evolution time has been $T_{\mathrm{evol}} = 10\,\mathrm{s}$ for each of the eight cycles and the cooling time has been $T_{\mathrm{cool}} = 45\,\mathrm{s}$. Additionally, there was a transport time of 80 s to swap the two ions.

4.1 Statistical uncertainty

Virtually the complete statistical uncertainty of one measurement cycle arises from the two successive modified cyclotron frequency measurements by the PnA method, see Fig. 4.1. One PnA cycle consists of around 45 s of cooling the modified cyclotron mode. This is followed by the imprinting of the modified cyclotron phase via a dipole excitation at the beginning of the phase measurement (T_{start}). During this excitation, the modified cyclotron radius is increased from the thermal radius of 4 μm to $r_+^{\mathrm{exc}} = 10\,\mu\mathrm{m}$ or in some cases up to $r_+^{\mathrm{exc}} = 60\,\mu\mathrm{m}$. After that, the cyclotron mode evolves for a certain time (T_{evol}). Finally, the modified cyclotron phase is transferred to the axial phase via a quadrupole excitation. In the last step the signal is read out (T_{end}). A detailed description of the PnA method can be found in [117]. The jitters occurring during the three different sections of the PnA measurement are discussed here.

Imprinting jitter at T_{start}

Before the imprinting of the phase, the motion of the particle is in thermal equilibrium with the detection system. Therefore, the amplitude of the modified cyclotron motion follows a thermal distribution and correspondingly the phase of the particle. The jitter of imprinting the phase for a certain temperature is approximately normally distributed for a typical dipole excitation to $r_+^{\mathrm{exc}} = 10\,\mu\mathrm{m}$ [117]. This imprinting jitter can be reduced by a larger dipole excitation. However, we want to measure the ion's rest mass and thus its cyclotron frequency at excitation energies as low as possible to minimize systematic shifts.

Readout jitter at T_{end}

An additional so-called technical readout jitter occurs during the readout of the axial phase, which depends on the signal-to-noise ratio of the readout signal and is ion-independent for similar measurement times and normally distributed, too [117]. This jitter is proportional to the excited axial amplitude. Here, our doubly compensated seven Penning trap enables us to reduce this jitter significantly. Further information are provided in section 3 of the second paper, see chapter 3.2.

Jitter during T_{evol}

Additionally, a phase jitter due to a jittering frequency occurs during the evolution time. Firstly, a jitter occurs due to the limited magnetic field stability. This is not normally distributed; rather it is assumed to have a random walk distribution. Further information are provided in section 3 of the second paper, see chapter 3.2.

Since the energy of the particle is approximately normally distributed after our dipole excitation, an additional frequency jitter occurs due to the relativistic mass increase and the B_2 inhomogeneity for subsequent PnA cycles. The corresponding frequency shifts are given by [156, 157]:

$$\Delta\nu_+|_{\text{Spec. relat.}} \approx -\frac{(2\pi)^2}{2}\frac{\nu_+^3}{c^2}\left(r_+^{\text{exc}}\right)^2 \quad , \tag{4.1}$$

$$\Delta\nu_+|_{B_2} \approx \frac{1}{2}\frac{\nu_+\nu_z}{B_0\nu_-}\left(r_+^{\text{exc}}\right)^2 \quad . \tag{4.2}$$

The jitter results from the product of the corresponding frequency shift with the evolution time. Thus these jitters increase linearly during T_{evol} and are approximately normally distributed, too. The width of the energy distribution and herewith this jitter can be reduced by smaller modified cyclotron excitation radius and a smaller initial thermal temperature of the ion.

An additional random walk can occur due to the voltage fluctuation on the trap electrodes during the evolution time. During the proton mass campaign an axial frequency jitter of $\delta\nu_z/\nu_z = 1 \times 10^{-7}$ over 5 min has been observed, which results in a jitter of 3×10^{-11} for ν_{c}. Therewith, this jitter has not been limiting the precision during the proton mass campaign. Further information are provided in section 4 of the second paper, see chapter 3.2.

Measurement of the combined jitter

The normally distributed phase jitters occurring at T_{start} and T_{end} can be measured as well as simulated. Furthermore, the frequency jitter due to special relativity and the B_2 inhomogeneity can be predicted by simulation, too. However, the temporal magnetic field jitter during T_{evol} is hard to specify. Only the combination of the magnetic field jitter and the other approximately normally distributed jitters arising during the PnA method can be measured and are shown in Fig 4.2, which also reflects the uncertainty of the determination of the modified cyclotron frequency.

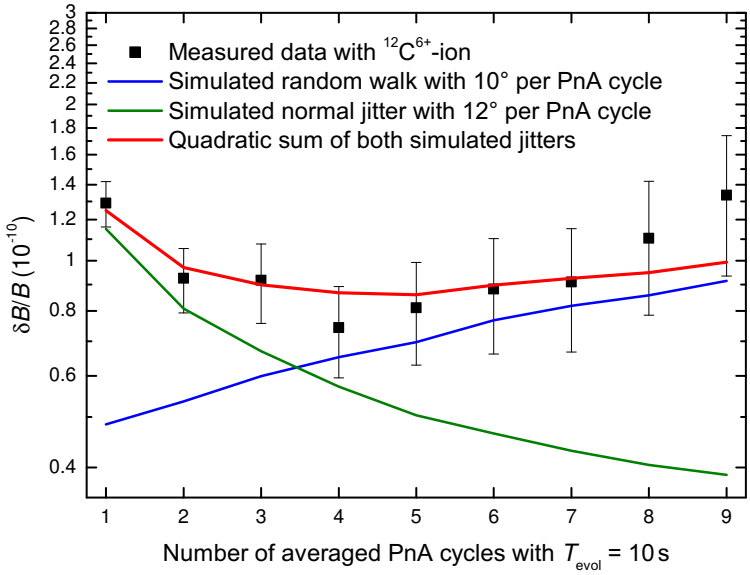

Figure 4.2: Allan deviation for different numbers of averaged phases of PnA cycles with $T_{\mathrm{evol}} = 10\,\mathrm{s}$ of a $^{12}C^{6+}$-ion. Furthermore, the trend of simulated normally distributed jitters caused by the imprinting of the phase, the readout of the phase and by a jittering modified cyclotron frequency together with special relativity and B_2 is shown in green. Additionally, a simulated random walk caused by temporal magnetic field fluctuations is plotted in blue. The quadratic sum of both jitters is plotted in red. After averaging over four PnA cycles, the uncertainty of the measured magnetic field decreases and reaches a minimum. For a larger number of averaging cycles the uncertainty increases due to the random walk of the magnetic field B. One PnA cycle consists of 10 s evolution time and 45 s cooling time.

The combination of all jitters is given by:

$$\frac{\delta B}{B} = \frac{\delta \nu_c}{\nu_c} \approx \frac{\delta \nu_+}{\nu_+} = \frac{\delta \phi_+}{\phi_+} = \frac{\delta \phi_+}{360° \nu_+ T_{\mathrm{evol}}} \quad , \tag{4.3}$$

$$\delta \phi_+ = \mathrm{std}\left(\phi_+\right) = \frac{\mathrm{std}\left(\mathrm{diff}\left(\phi_+^i, \phi_+^{i+1}\right)\right)}{\sqrt{2}} \quad , \tag{4.4}$$

where $\delta\phi_+$ is the jitter of the total modified cyclotron phase in degrees between subsequent i and $i+1$ modified cyclotron frequency phase measurements. The magnetic field stability $\delta B/B$ is measured via the repetition of several PnA cycles with $T_{\mathrm{evol}} = 10\,\mathrm{s}$. Further information are provided in section 3 of the second paper, see chapter 3.2.

The uncertainty of the normally distributed jitters can be reduced by averaging over multiple cycles, whereas the uncertainty due to random walk of the magnetic

field drift increases over time. The Allan deviation is a proper tool to decide for the optimal number of averaged cycles to reach the highest precision. At our Allan deviation plot the standard deviation of subsequent phase measurements is plotted for different numbers of averaged PnA cycles.

After four cycles the minimum of the Allan deviation is reached for our PnA cycle parameters. Therefore, for both ions the longest evaluation time of 10 s is averaged for four repetitions to get the most precise measurement of the modified cyclotron frequency with a relative jitter of 8×10^{-11} on average for one ion. After averaging four times, the normal distributed jitters have averaged down, and the change of the magnetic field is still comparably small. For longer evolution times and a larger number of averaged cycles, the random walk as well as the drift of the magnetic field increase and start to dominate the overall jitter. Therewith, the Allan deviation increases with a larger number of averaged PnA cycles, resulting in an equal or less precise determination of ν_+ for the ions. Further information are given in section 3 of the second paper, see chapter 3.2.

For the proton mass campaign, the total statistical uncertainty is 1.8×10^{-10} per measurement cycle. This is the standard deviation of all approximately 400 measured $\mathcal{R}^{\mathrm{CF}}$s for each run during the complete measurement campaign. This uncertainty arises due to two measurements of the modified cyclotron frequency. In between, there is a transport time to swap the ions in the PT, leading to a new setting of the voltages, which also contributes to the statistical uncertainty. Further information are given in section 4 of the second paper, see chapter 3.2.

4.2 Improving the statistical uncertainty

The jitters occurring at T_{start} and T_{end} are basically understood and can be reduced to reach stabilities in the order of 6°. These can be measured by choosing $T_{\mathrm{evol}} = 10\,\mathrm{ms}$. For such short evolution times, the result is mostly dominated by the imprinting and the readout jitter. Since these two are under control and their effect can be reduced with longer evolution times, the main focus is to improve on the frequency based jitters occurring during the long evolution time. There the jitter is between 25° to 35° for $T_{\mathrm{evol}} = 10\,\mathrm{s}$. Since there are several types of jitters contributing during T_{evol}, different approaches are necessary to reduce them.

Magnetic field stability

Magnetic field drifts and jitter can be caused by temperature fluctuations which change the magnetic susceptibility of the material surrounding the trapped ion. These temporal fluctuations can be reduced by pressure stabilization of the helium and nitrogen reservoir of the magnet as well as the respective reservoirs of the apparatus. With a currently developed pressure stabilization system it is possible to stabilize the pressure in all four reservoirs close to ambient pressure ($p = 1050\,\mathrm{mbar}$) with a stability of a few μbar. Preliminary measurements indicate that in this way it is possible to reach a factor of two more stable magnetic field [158].

Special relativity and B_2 jitter

To reduce the approximately normally distributed jitter due to the special relativity and the B_2 jitter during the evolution time, based on the initial thermal distribution of the ion, a colder particle will help. Additionally, this effect is especially large for the proton with its small mass, since it is given by:

$$\left.\frac{\delta\nu_+}{\nu_+}\right|_{\text{relativistic}} \approx -\frac{k_\text{B}T_+}{mc^2} \quad . \tag{4.5}$$

During the proton mass campaign, the axial temperature was cooled by the application of negative feedback to 1.5 K for the proton, resulting in a temperature of 116 K for the modified cyclotron frequency of the proton after sideband cooling. By using a modified cyclotron resonator it should be possible to cool the modified cyclotron mode to 4 K or even lower by applying negative feedback. Such resonators for the proton and the carbon ion were already implemented during the proton mass campaign, however their quality factors have been too low to achieve sufficiently short cooling times. The quality factors for the proton and the carbon ion were around 300, resulting in cooling time constants of more than 100 s. In the future a quality factor of both resonators larger than 2000 is necessary to achieve sufficiently fast cooling. Additionally, there are first attempts at other high-precision Penning-trap experiments to perform laser cooling of beryllium ions and couple their motion with the ones of the ion of interest for cooling them to temperature in the millikelvin regime [159, 160]. In the future similar techniques could be applied for the LIONTRAP experiment, too.

Axial jitter

Up to now, two different sources have been identified for the axial frequency jitter. Firstly, mechanical tilt fluctuations ($\delta\theta$) of the electrostatic quadrupole potential with respect to the magnetic field of the superconducting magnet lead to fluctuations of the observed axial frequency [141, 161]:

$$\nu_z \propto \sqrt{1-\frac{3}{2}\theta^2} \qquad \text{for small tilts } \theta \text{ and } \delta\theta: \qquad \delta\nu_z \propto \frac{3}{2}\theta\delta\theta \quad . \tag{4.6}$$

Secondly, also fluctuations of the voltage supply contribute to the axial jitter, which could be due to temperature fluctuations of the voltage references. The first reason has been addressed in the meantime. For the upcoming deuteron mass measurement, an elaborate mechanical mechanism to adjust the tilt has been commissioned. Therewith, it is possible to cancel the effect due to the tilt to a large extent; even if the fluctuations are similar, their effect on the axial frequency is reduced, see Eq. 4.6, since the axial jitter scales linear with the absolute tilt.

By addressing all these improvements, a relative statistical uncertainty below 10^{-10} per cycle should be possible.

4.3 Simultaneous $\mathcal{R}^{\mathrm{CF}}$ measurement scheme for non-doublets

In the current measurement scheme the modified cyclotron frequency of the two ions is determined in subsequent measurements. The more ideal case is that both cyclotron frequencies are measured simultaneously. This has already been shown for doublets via the ion balance [145]. However, it is not feasible to perform the ion balance scheme for non-doublets, like the proton and the carbon ion, because the ion separation would have to be overly small to achieve a coupling of the magnetron modes, which have significantly different frequencies due to the q/m mismatch. This small separation would lead to large systematic shifts arising from the mutual Coulomb interaction.

To overcome the magnetic field fluctuations, which limit our statistics, we will implement an extended measurement scheme in the second phase of LIONTRAP. To realize this, another approach will be used: an additional so-called magnetometer trap is introduced with a third so-called magnetometer ion ($\mathrm{I}_{\mathrm{mag}}$) to measure the phases of the reference ion, stored in the MT, and the proton, stored in the PT, simultaneously in a first step ($\mathcal{R}_1^{\mathrm{CF}}$), see Fig. 4.3.

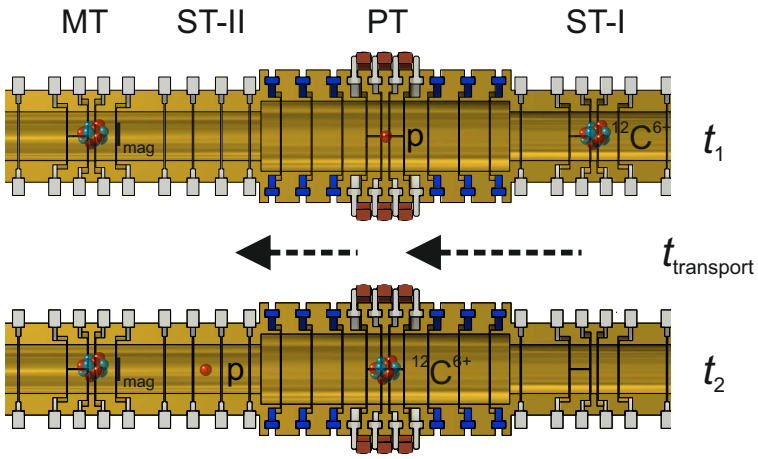

Figure 4.3: Principle of the simultaneous measurement scheme for non-doublets. In the first step, at time t_1 the $\mathcal{R}_1^{\mathrm{CF}}$ of the proton and the magnetometer ion ($\mathrm{I}_{\mathrm{mag}}$) is determined. This is followed by a swap of the ions in the PT. In the second step, at time t_2 the $\mathcal{R}_2^{\mathrm{CF}}$ of the carbon ion and the magnetometer ion is determined. Finally, the ratio of both $\mathcal{R}^{\mathrm{CF}}$s yields the sought after $\mathcal{R}^{\mathrm{CF}*}\left(\mathrm{p},{}^{12}\mathrm{C}^{6+}\right)$ of the proton and carbon ion. With such a measurement scheme all common-mode magnetic field fluctuations cancel out to a large extent. The figure is reproduced from [53].

In a second step, the carbon ion is transported into the PT and the phases of the carbon ion and the reference ion are measured simultaneously ($\mathcal{R}_2^{\mathrm{CF}}$). Dividing

$\mathcal{R}_1^{\mathrm{CF}}$ and $\mathcal{R}_2^{\mathrm{CF}}$ yields the sought after frequency ratio of the proton and the carbon ion, and all common-mode magnetic field fluctuations cancel out to a large extent. Consequently, the reference ion should be stored as close as possible to the PT, so that the magnetic field drift affects both ions in a similar way.

The time between the $T_{\mathrm{evol}} = 10\,\mathrm{s}$ measurements of the PnA method is around five minutes. During this time the magnetic fields change to $B_{\mathrm{PT}}(t_2) = B_{\mathrm{PT}}(t_1) + \Delta B_{\mathrm{PT}}$ and $B_{\mathrm{MT}}(t_2) = B_{\mathrm{MT}}(t_1) + \Delta B_{\mathrm{MT}}$, respectively. The $\mathcal{R}^{\mathrm{CF}}$ for the simultaneous phase-sensitive measurement scheme of the proton and carbon ion is derived in the following way:

$$\mathcal{R}_1^{\mathrm{CF}}\left(\mathrm{p}, \mathrm{I}_{\mathrm{mag}}, t_1\right) = \frac{\nu_c\left(\mathrm{p}, t_1\right)}{\nu_c\left(\mathrm{I}_{\mathrm{mag}}, t_1\right)} = \frac{q\left(\mathrm{p}\right) m\left(\mathrm{I}_{\mathrm{mag}}\right)}{m\left(\mathrm{p}\right) q\left(\mathrm{I}_{\mathrm{mag}}\right)} \frac{B_{\mathrm{PT}}\left(t_1\right)}{B_{\mathrm{MT}}\left(t_1\right)}, \tag{4.7}$$

$$\mathcal{R}_2^{\mathrm{CF}}\left({}^{12}\mathrm{C}^{6+}, \mathrm{I}_{\mathrm{mag}}, t_2\right) = \frac{\nu_c\left({}^{12}\mathrm{C}^{6+}, t_2\right)}{\nu_c\left(\mathrm{I}_{\mathrm{mag}}, t_2\right)} = \frac{q\left({}^{12}\mathrm{C}^{6+}\right) m\left(\mathrm{I}_{\mathrm{mag}}\right)}{m\left({}^{12}\mathrm{C}^{6+}\right) q\left(\mathrm{I}_{\mathrm{mag}}\right)} \frac{B_{\mathrm{PT}}\left(t_2\right)}{B_{\mathrm{MT}}\left(t_2\right)} \quad , \tag{4.8}$$

$$\mathcal{R}^{\mathrm{CF}*}\left(\mathrm{p}, {}^{12}\mathrm{C}^{6+}\right) = \frac{\mathcal{R}_1^{\mathrm{CF}}\left(\mathrm{p}, \mathrm{I}_{\mathrm{mag}}, t_1\right)}{\mathcal{R}_2^{\mathrm{CF}}\left({}^{12}\mathrm{C}^{6+}, \mathrm{I}_{\mathrm{mag}}, t_2\right)} \tag{4.9}$$

$$= \frac{\nu_c\left(\mathrm{p}, t_1\right)}{\nu_c\left(\mathrm{I}_{\mathrm{mag}}, t_1\right)} \frac{\nu_c\left(\mathrm{I}_{\mathrm{mag}}, t_2\right)}{\nu_c\left({}^{12}\mathrm{C}^{6+}, t_2\right)} \tag{4.10}$$

$$= \frac{q\left(\mathrm{p}\right) m\left({}^{12}\mathrm{C}^{6+}\right)}{m\left(\mathrm{p}\right) q\left({}^{12}\mathrm{C}^{6+}\right)} \frac{B_{\mathrm{PT}}\left(t_1\right) B_{\mathrm{MT}}\left(t_2\right)}{B_{\mathrm{MT}}\left(t_1\right) B_{\mathrm{PT}}\left(t_2\right)} \tag{4.11}$$

$$= \frac{q\left(\mathrm{p}\right) m\left({}^{12}\mathrm{C}^{6+}\right)}{m\left(\mathrm{p}\right) q\left({}^{12}\mathrm{C}^{6+}\right)} \frac{B_{\mathrm{PT}}\left(t_1\right)}{B_{\mathrm{MT}}\left(t_1\right)} \frac{B_{\mathrm{MT}}\left(t_1\right) + \Delta B_{\mathrm{MT}}}{B_{\mathrm{PT}}\left(t_1\right) + \Delta B_{\mathrm{PT}}}. \tag{4.12}$$

The factors containing the different magnetic fields and their variations are estimated to evaluate the effectiveness of the cancellation of the field effects, which arise during the determination of $\mathcal{R}^{\mathrm{CF}*}\left(\mathrm{p}, {}^{12}\mathrm{C}^{6+}\right)$. The distance between the PT and the MT is $d_{\text{PT-MT}} = 4\,\mathrm{cm}$ and the measured relative difference of B_0 between the PT and the MT is $B_{\mathrm{PT}} - B_{\mathrm{MT}} \approx 2 \times 10^{-4}\,\mathrm{T}$. Furthermore, it is assumed that all disturbances, which typically originate several $d_{\text{PT-MT}}$ away from these traps, result in common-mode magnetic field fluctuations. A typical value for the PT, observed during the proton mass measurement campaign, was $\Delta B_{\mathrm{PT}} = \Delta B_{\mathrm{MT}} = 8 \times 10^{-10}\,\mathrm{T}$ for a time span of five minutes, which yields:

$$\frac{B_{\mathrm{PT}}\left(B_{\mathrm{MT}} + \Delta B_{\mathrm{MT}}\right)}{B_{\mathrm{MT}}\left(B_{\mathrm{PT}} + \Delta B_{\mathrm{PT}}\right)} - 1 \approx \frac{\Delta B_{\mathrm{PT}}}{B_{\mathrm{PT}}} \frac{B_{\mathrm{PT}} - B_{\mathrm{MT}}}{B_{\mathrm{PT}}} = 1 \times 10^{-14} \quad . \tag{4.13}$$

An additional statistical effect of 1×10^{-14} arises due to the different magnetic fields in the PT and the MT and their common-mode change. By implementing this new measurement scheme, the phase evolution times could be even longer and, therefore, the statistical uncertainty per measurement cycle could be improved even more.

First preliminary experiments have been conducted by applying this new measurement scheme. However, up to now it has not been possible to measure coherent phases for two identical ions in both traps at evolution times of 10 s or longer. The reason for this is unclear up to now. One possibility could be a material with a strong temperature-dependent magnetic susceptibility, located very close to one of the two traps. For such a case the magnetic field fluctuation would be different within the two traps.

4.4 Systematic uncertainties

In total three systematic uncertainties are responsible for the complete systematic uncertainty for the proton mass measurement. In the following section the corresponding effects are presented as well as methods to reduce their uncertainties.

Quadratic magnetic field inhomogeneity

The systematic uncertainty due to the magnetic inhomogeneity B_2 and the finite axial temperature T_z of the ion lead to the largest uncertainty during the proton mass campaign and is given by:

$$\langle B \rangle = B_0 + B_2 \frac{k_\mathrm{B} T_z}{m \left(2\pi\nu_z\right)^2} \quad . \tag{4.14}$$

Due to its small mass, the cyclotron frequency of the proton is mainly shifted due to this effect. To reduce this, a special superconducting closed B_2 shim coil has been wound, see Fig. 4.4. First preliminary measurements suggest that it is possible to reduce the quadratic magnetic field component in the PT by more than a factor of one hundred. Therefore, for the upcoming measurements this uncertainty should be drastically reduced. Further information are provided in section 4 of the second paper, see chapter 3.2.

Finite axial temperature

In the proton mass campaign the finite axial temperature contributed to the systematic shift with a budget of 71 ppt due to the special relativity extrapolation to zero energy. This shift and the corresponding uncertainty will be reduced by colder particles via the application of modified cyclotron resonators or other cooling methods, as discussed in section 4.2. Further information are provided in section 4 of the second paper, see chapter 3.2.

Image charge effect

The image charge effect causes the largest systematic shift, which has been measured to a precision of 5 %, see chapter 3.3. However, further improvement is necessary to diminish this effect. During the next image charge measurement

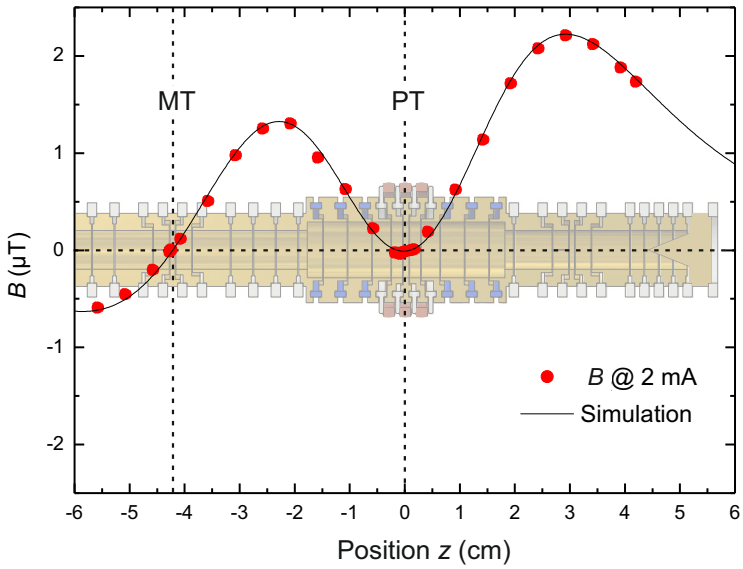

Figure 4.4: Offline measured magnetic field of the B_2 shim coil along the z-axis at $x = y = 0$. The red dots symbolize the measured data, whereas the black curve arises from simulations. The generated B_2/I at the PT is around $3.5\,\mathrm{nT/(mm^2{\cdot}mA)}$. The measurement has been done at room temperature with a Hall effect sensor. The measurement and the simulation are in good agreement. In the background the position of the trap tower in a relation to the shim coil is shown. At the center of the PT and the MT, the generated magnetic field is close to zero to avoid undesired effects due to a potentially generated large and unstable B_0. The figure is reproduced from [53].

the magnetron frequency of carbon and deuterium will be compared. This reduces some systematic uncertainties, since these two ions are a q/m doublet. The largest uncertainty of the measurement of the image charge effect originated from the tilt of the electrostatic quadrupole potential in comparison to the magnetic field. This effect and therewith its uncertainty can be drastically reduced in the following measurement, since it is now possible to reduce the tilt by more than one order of magnitude. Therewith, the systematic uncertainty of the measurement can be reduced by an order of magnitude. Thus, it should be possible to measure the image charge shift with a relative precision of 2% during the upcoming measurement campaign.

4.5 Conclusion

With all these exciting new upgrades it should be possible to measure the atomic masses of deuteron, triton and helion with a lower uncertainty compared to the

most recent CODATA values and thus to provide an important internal consistency check for the KATRIN experiment. Additionally, with these measurements it should be possible to address the light ion mass puzzle and resolve its five sigma discrepancy.

Furthermore, it is also possible to determine the atomic masses of other important light nuclei with a ppt relative uncertainty starting with the deuteron. Preliminary measurements suggest a total systematic relative uncertainty below 6×10^{-12} for the deuteron mass. On the other hand a more precise deuteron mass together with an improved measurement of the nuclear binding energy of the deuteron leads to a new high precision determination of the neutron mass.

5 Summary

In this thesis the new high-precision mass spectrometer LIONTRAP has been introduced. It has been designed for the determination of the atomic masses of light ions. The apparatus consists of five traps, among others the precision trap, which generates the most harmonic electrostatic quadrupole potential of an ion trap described in literature so far.

Furthermore, it has been possible to accomplish the first phase sensitive measurement of a single proton with this new mass spectrometer. For the first time, two detection systems for the ions' axial motion have been connected to one trap, which allowed us to measure the axial frequency of ions with a charge-to-mass ratio different by a factor of two without changing the voltage of the trap.

Additionally, the whole commissioning of the new experiment is described in detail: the determination of the magnetic field stability, magnetic field inhomogeneity as well as the ion temperatures. It is shown that the combined systematic uncertainties are at a level of 3×10^{-11}.

During this time the LIONTRAP experiment enabled two major measurement campaigns. In the first campaign, the atomic mass of the proton has been measured to:

$$m_\mathrm{p} = 1.007\,276\,466\,598\,(33)\,\mathrm{u} \quad . \tag{5.1}$$

This is a factor of three more precise compared to the literature value from CODATA 2014, revealing a three sigma deviation from it. Our measurement value of the proton mass is smaller than the one from CODATA 2014 and is included in the recent literature value of the CODATA evaluation from 2018 [102]:

$$m_\mathrm{p}\,(\mathrm{CODATA\ 2018}) = 1.007\,276\,466\,621\,(53)\,\mathrm{u} \quad . \tag{5.2}$$

Accordingly, our result shifted the literature value and is in accordance with the current one. Additionally, the atomic mass of oxygen has been measured with the second best precision so far:

$$m\left(^{16}\mathrm{O}\right) = 15.994\,914\,619\,37\,(87)\,\mathrm{u} \quad . \tag{5.3}$$

This result is in accordance with the current literature value.

In a second measurement campaign the image charge shift has been experimentally measured for the LIONTRAP setup with an uncertainty of 5%. This is again the second most precise relative measurement of this shift. Additionally, the arising shift was simulated and the result is in accordance with the experimentally determined one.

Furthermore, first steps to improve the current results are presented. The largest systematic uncertainty arises from the quadratic magnetic field inhomogeneity in combination with the finite ion temperature. A superconducting shim coil has been wound and tested to compensate the inhomogeneity of the magnet. First preliminary tests suggest a reduction of the quadratic magnetic field inhomogeneity by a factor of one hundred. Additionally, the concept of the simultaneous phase sensitive measurement and the pressure stabilization of the helium reservoirs of the experiment is under way to further reduce the systematic uncertainty. Preliminary tests suggest an improvement of a factor of two in stability by applying pressure stabilization.

Since there is a lasting inconsistency between light ion masses, these masses can be measured with a relative statistical and systematical uncertainty at the ppt level at the LIONTRAP experiment in the future. With this exciting outlook I conclude my thesis.

Bibliography

[1] F. Clarke, The Constants of Nature, Pt. 5 - Recalculation of the atomic weights, Smithsonian Miscellaneous Publications No. 441, 1882.

[2] F. H. Wallaston, A Synoptic scale of chemical equivalents, Philos. Trans. R. Soc. London (1814) 20.

[3] J. Berezlius, P. L. Dulong, Ann. Philos. (1821) 48.

[4] T. Thomson, Bemerkungen über die Atomengewichte der Körper, Erdmann's Journ. Prak. Chem. (1) (1836) 359.

[5] R. D. Thomson, Records of General Science, Taylor and Walton, 1836.

[6] J. Dumas, Compt. Rend. (1842) 537.

[7] J. Dumas, Compt. Rend. (1841) 1005.

[8] H. V. Regnault, Compt. Rend. (1845) 975.

[9] T. W. Richards, J. P. Cooke, The relative values of the atomic weights of hydrogen and oxygen, Am. Chem. J. (1888) 81.

[10] O. L. Erdmann, R. F. Marchand, Ueber die Atomgwichte des Wasserstoffes und des Calciums, Erdmann's Journ. Prak. Chem. (1) (1842) 461.

[11] J. Thomsen, Ueber einige Constanten des Wasserstoffs und des Sauerstoffs, Ber. Dtsch. Chem. Ges. (2) (1870) 928.

[12] F. W. Clarke, On the densities of Oxygen and Hydrogen, and on the ratio of their atomic weights, J. Am. Chem. Soc. (1896) 192.

[13] W. A. Noyes, On the Densities of Oxygen and Hydrogen and on the Ratio of their Atomic Weights, Science 3 (53) (1896) 25.

[14] F. W. Aston, The mass-spectra of chemical elements, Philos. Mag. 39 (233) (1920) 611.

[15] F. W. Aston, Isotopes and Atomic Weights, Nature (1920) 617.

[16] F. W. Aston, Bakerian Lecture: A new mass-spectrograph and the whole number rule, Proc. R. Soc. London Ser. A 115 (772) (1927) 487.

[17] F. W. Aston, Masses of some Light Atoms measured by means of a New Mass-Spectrograph, Nature (1936) 357.

[18] F. W. Aston, A second-order focusing mass spectrograph and isotopic weights by the doublet method, Proc. R. Soc. London Ser. A 163 (914) (1937) 391.

[19] K. T. Bainbridge, Comparison of the Masses of He and H^1 on a Mass-Spectrograph, Phys. Rev. 43 (1933) 103.

[20] J. Mattauch, A Double-Focusing Mass Spectrograph and the Masses of N^{15} and O^{18}, Phys. Rev. 50 (1936) 617.

[21] J. Mattauch, Discussion on the Isotopic Weight of C^{12}, Phys. Rev. 57 (1940) 1155.

[22] J. Mattauch, R. Bieri, Eine massenspektrographische Neubestimmung der Massen von ^{1}H, ^{2}D, ^{4}He, ^{12}C und ^{14}N, Z. Naturforsch. A (1954) 303.

[23] K. T. Bainbridge, E. B. Jordan, Minutes of the Atlantic City Meeting, December 28-30, 1936, Phys. Rev. 51 (1937) 373.

[24] K. T. Bainbridge, The Isotopic Weight of Helium, Phys. Rev. 81 (1951) 146.

[25] A. O. Nier, The Atomic Masses of H^1, C^{12}, and S^{32}, Phys. Rev. 81 (1951) 624.

[26] T. L. Collins, A. O. Nier, W. H. Johnson, Atomic Masses in the Region about Mass 40, Phys. Rev. 84 (1951) 717.

[27] K. S. Quisenberry, T. T. Scolman, A. O. Nier, Atomic Masses of H^1, D^2, C^{12}, and S^{32}, Phys. Rev. 102 (1956) 1071.

[28] K. S. Quisenberry, C. F. Giese, J. L. Benson, Atomic Masses of H^1, C^{12}, and S^{32}, Phys. Rev. 107 (1957) 1664.

[29] J. L. Benson, W. H. Johnson, Isotopic Masses of Hydrogen, Chlorine, Barium, Cerium, and Neodymium, Phys. Rev. 141 (1966) 1112.

[30] K. Ogata, H. Matsuda, Masses of Light Atoms, Phys. Rev. 89 (1953) 27.

[31] H. Matsuda, T. Matsuo, Atomic Masses of ^{1}H, ^{16}O and ^{32}S, J. Phys. Soc. of JPN. 25 (4) (1968) 950.

[32] I. Katakuse, H. Nakabushi, K. Ogata, Preliminary Report on the Atomic Masses of H, D and ^{35}Cl, J. Mass Spectrom. Soc. JPN 18 (4) (1970) 1276.

[33] E. Heinz, Die Massen der Substandards ^{1}H, ^{2}D, ^{12}C und anderer leichter Atome (1951) 293.

[34] C. M. Stevens, P. E. Moreland, Proceedings of the Third International Conference on Atomic Masses (1967) 673.

[35] C. M. Stevens, P. E. Moreland, Proceedings of the International Conference in Mass Spectroscopy, Kyoto (1970) 1296.

[36] R. A. Demirkhanov, T. I. Gutkin, V. V. Dorokhov, A. D. Rudenko, Masses of the H, D, He4 and C12 isotopes, Sov. J. At. En. 1 (2) (1956) 163.

[37] L. G. Smith, Measurements of Light Masses with the Mass Synchrometer, Phys. Rev. 111 (1958) 1606.

[38] L. Friedman, W. Henkes, D. Christman, C^{14}-N^{14} Mass Difference and Mass Excesses of Some Light Nuclides, Phys. Rev. 115 (1959) 166.

[39] L. G. Smith, Measurements of Six Light Masses, Phys. Rev. C 4 (1971) 22.

[40] R. S. Van Dyck, F. L. Moore, D. L. Farnham, P. B. Schwinberg, Mass ratio spectroscopy and the proton's atomic mass, in: Frequency Standards and Metrology, Springer Berlin Heidelberg, 1989, p. 349.

[41] R. S. Van Dyck Jr., D. L. Farnham, P. B. Schwinberg, High precision penning trap mass spectroscopy of the light ions, in: 6th International Conference on Nuclei Far from Stability (NFFS 6) Jointly with 9th International Conference on Atomic Masses and Fundamental Constants (AMCO 9), 1992, p. 3.

[42] R. S. Van Dyck Jr., D. L. Farnham, P. B. Schwinberg (1993) 946.

[43] R. S. van Dyck, D. L. Farnham, P. B. Schwinberg, Precision mass measurements in the UW-PTMS and the electron's atomic mass, Phys. Scr. T59 (1995) 134.

[44] R. S. Van Dyck Jr., D. L. Farnham, S. L. Zafonte, P. B. Schwinberg, High precision Penning trap mass spectroscopy and a new measurement of the proton's atomic mass, AIP Conf. Proc. 457 (1) (1999) 101.

[45] V. Natarajan, K. R. Boyce, F. DiFilippo, D. E. Pritchard, Precision Penning trap comparison of nondoublets: Atomic masses of H, D, and the neutron, Phys. Rev. Lett. 71 (1993) 1998.

[46] F. DiFilippo, V. Natarajan, K. R. Boyce, D. E. Pritchard, Accurate Atomic Masses for Fundamental Metrology, Phys. Rev. Lett. 73 (1994) 1481.

[47] F. DiFilippo, V. Natarajan, M. Bradley, F. Palmer, D. E. Pritchard, Accurate atomic mass measurements from Penning trap mass comparisons of individual ions, Phys. Scr. T59 (1995) 144.

[48] H. Borgenstrand, Ph.D. thesis, Stockholm University (1997).

[49] C. Carlberg, Mass measurements of few-electron systems in Penning traps, Hyperfine Interact. 114 (1) (1998) 177.

[50] I. Bergström, T. Fritioff, R. Schuch, J. Schönfelder, On the Masses of ^{28}Si and the Proton Determined in a Penning Trap, Phys. Scr. 66 (3) (2002) 201.

[51] A. Solders, I. Bergström, S. Nagy, M. Suhonen, R. Schuch, Determination of the proton mass from a measurement of the cyclotron frequencies of D^+ and H_2^+ in a Penning trap, Phys. Rev. A. 78 (2008) 012514.

[52] F. Heiße, F. Köhler-Langes, S. Rau, J. Hou, S. Junck, A. Kracke, A. Mooser, W. Quint, S. Ulmer, G. Werth, K. Blaum, S. Sturm, High-Precision Measurement of the Proton's Atomic Mass, Phys. Rev. Lett. 119 (2017) 033001.

[53] F. Heiße, S. Rau, F. Köhler-Langes, W. Quint, G. Werth, S. Sturm, K. Blaum, accepted by Phys. Rev. A (2019).

[54] J. Dalton, On the absorption of gases by water and other liquids, Mem. Proc. Manchr. Lit. Phil. Soc. (1805) 271.

[55] J. Dalton, New System of Chemical Philosophy Pt. I, S. Russell for R. Bickerstaff, 1808.

[56] H. Cavendish, Three papers, containing experiments on factitious air, Philos. Trans. R. Soc. London 56 (1766) 141.

[57] W. Prout, On the relation between the specific gravities of bodies in their gaseous state and the weights of their atoms, Ann. Philos. (1815) 321.

[58] W. Prout, Corrections of a mistake in the essay on the relation between the specific gravities of bodies in their gaseous state and the weights of their atoms, Ann. Philos. (1816) 111.

[59] J. Gay-Lussac, Memoire sur la combinaison des substances gazeuses, les unes avec les autres, Memoires de physique et de chemie de la Societe d'Acueil (1809) 207.

[60] A. Avogadro, Essai d'une maniere de determiner les masses relatives des molecules elementaires des corps, et les proportions selon lesquelles elles entrent dans ces combinaisons, J. Phys. (1811) 58.

[61] W. Hisinger, J. Berzelius, Forsok rorande de bestamda proportioner, havari den oorganiska naturens bestandsdelar finnas forenada, Afh. Fys., Kemi Mineral. (1810) 162.

[62] J. Dumas, J. Stas, Recherches sur le veritable poid atomique du carbone, Compt. Rend. (1840) 991.

[63] J. Stas, Recherches sur les rapports reciproques des poids atomiques, Bull. Acad. R. Belg. (1860) 208.

[64] J. Stas, Nouvelles recherches sur les lois des proportions chimiques, sur les poids atomiques et leurs rapports mutuels, Mem. Acad. R. Belg (1865) 3.

[65] D. Mendeleev, Correlation of the properties with the atomic weight of elements, J. Russ. Chem. Soc. (1869) 60.

[66] J. Meyer, Die modernen Theorien der Chemie und ihre Bedeutung fur die chemische Statistik, Maruschke and Berendt, 1864.

[67] T. B. Coplen, H. S. Peiser, History of the recommended atomic-weight values from 1882 to 1997: A comparison of differences from current values to the estimated uncertainties of earlier values (Technical Report), Pure Appl. Chem. (1998) 237.

[68] T. W. Richards, A Determination of the Relation of the Atomic Weights of Copper and Silver, Proc. American Acad. Sci. 22 (1886) 342.

[69] F. W. Clarke, Report of the international committee on atomic weights, J. Am. Chem. Soc. (1903) 1.

[70] F. W. Clarke, T. E. Thorpe, K. Seubert, H. Moissan, Report of the international committee on atomic weights, J. Chem. Soc. Abstr. 84 (1903) 1.

[71] F. W. Clarke, Report of committee on determinations of atomic weight, published during 1893, J. Am. Chem. Soc. (1894) 179.

[72] E. Goldstein, Ueber eine noch nicht untersuchte Strahlungsform an der Kathode inducirter Entladungen, Ann. Phys. 300 (1) (1898) 38.

[73] E. Goldstein, Sitzungsberichte der königlichen akademie der wissenschaften zu berlin (1886).

[74] W. Wien, Untersuchungen über die electrische Entladung in verdünnten Gasen, Ann. Phys. 301 (6) (1898) 440.

[75] J. J. Thomson, Cathode Rays, Philos. Mag. 44 (269) (1897) 293.

[76] J. J. Thomson, On rays of positive electricity, Philos. Mag. 13 (77) (1907) 561.

[77] J. Thomson, Further experiments on positive rays, Philos. Mag. 24 (140) (1912) 209.

[78] J. J. Thomson, Bakerian Lecture: Rays of positive electricity, Proc. R. Soc. London Ser. A 89 (607) (1913) 1.

[79] F. Soddy, The radio-elements and the periodic law, Chem. News (1913) 97.

[80] E. Rutherford, Collision of alpha particles with light atoms. IV. An anomalous effect in nitrogen, Philos. Mag. 37 (222) (1919) 581.

[81] E. Rutherford, The scattering of alpha and beta particles by matter and the structure of the atom, Philos. Mag. 21 (125) (1911) 669.

[82] N. Bohr, On the constitution of atoms and molecules, Philos. Mag. 26 (151) (1913) 1.

[83] F. Aston, A positive ray spectrograph, Philos. Mag. 38 (228) (1919) 707.

[84] A. S. Eddington, The Internal Constitution of the Stars, Nature (1920) 14.

[85] M. G. Mayer, On Closed Shells in Nuclei, Phys. Rev. 74 (1948) 235.

[86] A. J. Dempster, A new Method of Positive Ray Analysis, Phys. Rev. 11 (1918) 316.

[87] A. J. Dempster, Positive Ray Analysis of Lithium and Magnesium, Phys. Rev. 18 (1921) 415.

[88] A. J. Dempster, Positive-Ray Analysis of Potassium, Calcium and Zinc, Phys. Rev. 20 (1922) 631.

[89] R. Herzog, Ionen- und elektronenoptische Zylinderlinsen und Prismen. I, Z. Phys. 89 (7) (1934) 447.

[90] J. Mattauch, R. Herzog, Über einen neuen Massenspektrographen, Z. Phys. 89 (11) (1934) 786.

[91] A. J. Dempster, New Methods in Mass Spectroscopy, Proc. Am. Philos. Soc. 75 (8) (1935) 755.

[92] K. T. Bainbridge, E. B. Jordan, Mass Spectrum Analysis 1. The Mass Spectrograph. 2. The Existence of Isobars of Adjacent Elements, Phys. Rev. 50 (1936) 282.

[93] T. Asada, T. Okuda, K. Ogata, S. Yoshimoto, Physics and Chemistry: Preliminary Report on the Masses of ^{12}C and ^{14}N, Nature 143 (1939) 797.

[94] J. Mattauch, Discussion on the Isotopic Weight of C^{12}, Phys. Rev. 57 (1940) 1155.

[95] A. O. Nier, T. R. Roberts, The Determination of Atomic Mass Doublets by Means of a Mass Spectrometer, Phys. Rev. 81 (1951) 507.

[96] E. Heinz, Eine Neukonstruktion des Mattauch-Herzog'schen doppelfokussierenden Massenspektrographen, Z. Naturforsch. A (1946).

[97] L. G. Smith, A New Magnetic Period Mass Spectrometer, Rev. Sci. Instrum. 22 (2) (1951) 115.

[98] L. G. Smith, C. C. Damm, Mass Synchrometer, Rev. Sci. Instrum. 27 (8) (1956) 638.

[99] L. G. Smith, C. C. Damm, Mass Synchrometer Doublet Measurements at Masses 28 and 30, Phys. Rev. 90 (1953) 324.

[100] H. Dehmelt, Experiments with an isolated subatomic particle at rest, Rev. Mod. Phys. 62 (1990) 525.

[101] P. J. Mohr, D. B. Newell, B. N. Taylor, CODATA recommended values of the fundamental physical constants: 2014, Rev. Mod. Phys. 88 (2016) 035009.

[102] NIST Reference on Constants [accessed June 13, 2019].

[103] R. S. Westfall, The Life of Isaac Newton, Canto original series, Cambridge University Press, 1994.

[104] G. Audi, The history of nuclidic masses and of their evaluation, Int. J. Mass Spectrom. 251 (2) (2006) 85.

[105] A. H. Wapstra, Atomic masses: Thomson to ion traps, Phys. Scr. T59 (1995) 65.

[106] G. Münzenberg, Development of mass spectrometers from Thomson and Aston to present, Int. J. Mass Spectrom. 349-350 (2013) 9.

[107] N. E. Holden, Atomic Weights, Chem. Int. (2004) 4.

[108] KATRIN Collaboration, Katrin design report, Tech. rep. (2005).

[109] S. Hamzeloui, J. A. Smith, D. J. Fink, E. G. Myers, Precision mass ratio of $^3He^+$ to HD^+, Phys. Rev. A 96 (2017) 060501.

[110] S. L. Zafonte, R. S. Van Dyck Jr., Ultra-precise single-ion atomic mass measurements on deuterium and helium-3, Metrologia 52 (2) (2015) 280.

[111] Z.-C. Yan, J.-Y. Zhang, Y. Li, Energies and polarizabilities of the hydrogen molecular ions, Phys. Rev. A 67 (2003) 062504.

[112] E. Otten, Searching the absolute neutrino mass in tritium β-decay—interplay between nuclear, atomic and molecular physics, Hyperfine Interact. 196 (1) (2010) 3.

[113] S. Dürr, Z. Fodor, J. Frison, C. Hoelbling, R. Hoffmann, S. D. Katz, S. Krieg, T. Kurth, L. Lellouch, T. Lippert, K. K. Szabo, G. Vulvert, Ab Initio Determination of Light Hadron Masses, Science 322 (5905) (2008) 1224.

[114] S. Borsanyi, S. Dürr, Z. Fodor, C. Hoelbling, S. D. Katz, S. Krieg, L. Lellouch, T. Lippert, A. Portelli, K. K. Szabo, B. C. Toth, Ab initio calculation of the neutron-proton mass difference, Science 347 (6229) (2015) 1452.

[115] Y.-B. Yang, J. Liang, Y.-J. Bi, Y. Chen, T. Draper, K.-F. Liu, Z. Liu, Proton Mass Decomposition from the QCD Energy Momentum Tensor, Phys. Rev. Lett. 121 (2018) 212001.

[116] Sturm, S. and Köhler, F. and Zatorski, J. and Wagner, A. and Harman, Z. and Werth, G. and Quint, W. and Keitel, C. H. and Blaum, K., High-precision measurement of the atomic mass of the electron, Nature 506 (7489) (2014) 467.

[117] F. Köhler, S. Sturm, A. Kracke, G. Werth, W. Quint, K. Blaum, The electron mass from g -factor measurements on hydrogen-like carbon $^{12}C^{5+}$, J. Phys. B 48 (14) (2015) 144032.

[118] M. Hori, H. Aghai-Khozani, A. Sótér, D. Barna, A. Dax, R. Hayano, T. Kobayashi, Y. Murakami, K. Todoroki, H. Yamada, D. Horváth, L. Venturelli, Buffer-gas cooling of antiprotonic helium to 1.5 to 1.7 K, and antiproton-to-electron mass ratio, Science 354 (6312) (2016) 610.

[119] S. Alighanbari, M. G. Hansen, V. I. Korobov, S. Schiller, Rotational spectroscopy of cold and trapped molecular ions in the Lamb–Dicke regime, Nat. Phys. 14 (6) (2018) 555.

[120] M. S. Safronova, D. Budker, D. DeMille, D. F. J. Kimball, A. Derevianko, C. W. Clark, Search for new physics with atoms and molecules, Rev. Mod. Phys. 90 (2018) 025008.

[121] S. G. Karshenboim, V. G. Ivanov, Quantum electrodynamics, high-resolution spectroscopy and fundamental constants, Appl. Phys. B 123 (1) (2016) 18.

[122] C. G. Parthey, A. Matveev, J. Alnis, B. Bernhardt, A. Beyer, R. Holzwarth, A. Maistrou, R. Pohl, K. Predehl, T. Udem, T. Wilken, N. Kolachevsky, M. Abgrall, D. Rovera, C. Salomon, P. Laurent, T. W. Hänsch, Improved Measurement of the Hydrogen $1S - 2S$ Transition Frequency, Phys. Rev. Lett. 107 (2011) 203001.

[123] A. Antognini, F. Nez, K. Schuhmann, F. D. Amaro, F. Biraben, J. M. R. Cardoso, D. S. Covita, A. Dax, S. Dhawan, M. Diepold, L. M. P. Fernandes, A. Giesen, A. L. Gouvea, T. Graf, T. W. Hänsch, P. Indelicato, L. Julien, C.-Y. Kao, P. Knowles, F. Kottmann, E.-O. Le Bigot, Y.-W. Liu, J. A. M. Lopes, L. Ludhova, C. M. B. Monteiro, F. Mulhauser, T. Nebel, P. Rabinowitz, J. M. F. dos Santos, L. A. Schaller, C. Schwob, D. Taqqu, J. F. C. A. Veloso, J. Vogelsang, R. Pohl, Proton Structure from the Measurement of 2S-2P Transition Frequencies of Muonic Hydrogen, Science 339 (6118) (2013) 417.

[124] A. Beyer, L. Maisenbacher, A. Matveev, R. Pohl, K. Khabarova, A. Grinin, T. Lamour, D. C. Yost, T. W. Hänsch, N. Kolachevsky, T. Udem, The Rydberg constant and proton size from atomic hydrogen, Science 358 (6359) (2017) 79.

[125] H. Fleurbaey, S. Galtier, S. Thomas, M. Bonnaud, L. Julien, F. Biraben, F. Nez, M. Abgrall, J. Guéna, New Measurement of the $1S - 3S$ Transition Frequency of Hydrogen: Contribution to the Proton Charge Radius Puzzle, Phys. Rev. Lett. 120 (2018) 183001.

[126] S. Ulmer, C. Smorra, A. Mooser, K. Franke, H. Nagahama, G. Schneider, T. Higuchi, S. Van Gorp, K. Blaum, Y. Matsuda, W. Quint, J. Walz, Y. Yamazaki, High-precision comparison of the antiproton-to-proton charge-to-mass ratio, Nature (2015) 196.

[127] W. Huang, G. Audi, M. Wang, F. Kondev, S. Naimi, X. Xu, The AME2016 atomic mass evaluation (I). Evaluation of input data; and adjustment procedures, Chin. Phys. C 41 (3) (2017) 030002.

[128] M. Wang, G. Audi, F. G. Kondev, W. Huang, S. Naimi, X. Xu, The AME2016 atomic mass evaluation (II). Tables, graphs and references, Chin. Phys. C 41 (3) (2017) 030003.

[129] E. G. Kessler, M. S. Dewey, R. D. Deslattes, A. Henins, H. G. Börner, M. Jentschel, C. Doll, H. Lehmann, The deuteron binding energy and the neutron mass, Phys. Lett. A 255 (4) (1999) 221.

[130] M. S. Dewey, E. G. Kessler, R. D. Deslattes, H. G. Börner, M. Jentschel, C. Doll, P. Mutti, Precision measurement of the ^{29}Si, ^{33}S, and ^{36}Cl binding energies, Phys. Rev. C 73 (2006) 044303.

[131] Balancing energy and mass with neutrons, Nat. Phys. (2018) 524.

[132] S. Rainville, J. K. Thompson, E. G. Myers, J. M. Brown, M. S. Dewey, E. G. Kessler Jr, R. D. Deslattes, H. G. Börner, M. Jentschel, P. Mutti, D. E. Pritchard, A direct test of $E = mc^2$, Nature 438 (2005) 1096.

[133] J. Krempel, Ph.D. thesis, Ludwig-Maximilians-Universität München (2010).

[134] J. Repp, C. Böhm, J. R. Crespo López-Urrutia, A. Dörr, S. Eliseev, S. George, M. Goncharov, Y. N. Novikov, C. Roux, S. Sturm, S. Ulmer, K. Blaum, PENTATRAP: a novel cryogenic multi-Penning-trap experiment for high-precision mass measurements on highly charged ions, Appl. Phys. B 107 (4) (2012) 983.

[135] C. Roux, C. Böhm, A. Dörr, S. Eliseev, S. George, M. Goncharov, Y. N. Novikov, J. Repp, S. Sturm, S. Ulmer, K. Blaum, The trap design of PENTATRAP, Appl. Phys. B 107 (4) (2012) 997.

[136] E. G. Myers, A. Wagner, H. Kracke, B. A. Wesson, Atomic Masses of Tritium and Helium-3, Phys. Rev. Lett. 114 (2015) 013003.

[137] G. Drexlin, Direct neutrino mass searches, Nucl. Phys. B Proc. Suppl. 138 (2005) 282.

[138] S. Earnshaw, On the nature of the molecular forces which regulate the constitution of the luminiferous ether, Trans. Cambridge Philos. Soc. (1842) 97.

[139] G. Gabrielse, F. Mackintosh, Cylindrical Penning traps with orthogonalized anharmonicity compensation, Int. J. Mass Spectrom. 57 (1) (1984) 1.

[140] J. Verdú, Ph.D. thesis, Johannes Gutenberg-University Mainz (2003).

[141] L. S. Brown, G. Gabrielse, Precision spectroscopy of a charged particle in an imperfect Penning trap, Phys. Rev. A 25 (1982) 2423.

[142] A. Kramida, Yu Ralchenko, J. Reader and the NIST ASD Team [accessed May 17,2017].

[143] R. S. Van Dyck Jr., S. L. Zafonte, P. B. Schwinberg, Ultra-Precise Mass Measurements Using the UW-PTMS, Hyperfine Interact. 132 (1) (2001) 163.

[144] R. S. Van Dyck Jr., D. B. Pinegar, S. Van Liew, S. L. Zafonte, The UW-PTMS: Systematic studies, measurement progress, and future improvements, Int. J. Mass Spectrom. 251 (2) (2006) 231.

[145] S. Rainville, J. K. Thompson, D. E. Pritchard, An Ion Balance for Ultra-High-Precision Atomic Mass Measurements, Science 303 (5656) (2004) 334.

[146] R. S. Van Dyck Jr., S. L. Zafonte, S. Van Liew, D. B. Pinegar, P. B. Schwinberg, Ultraprecise Atomic Mass Measurement of the α Particle and ^{4}He, Phys. Rev. Lett. 92 (2004) 220802.

[147] W. Shi, M. Redshaw, E. G. Myers, Atomic masses of ^{32,33}S, ^{84,86}Kr, and ^{129,132}Xe with uncertainties , Phys. Rev. A 72 (2005) 022510.

[148] M. Redshaw, J. McDaniel, E. G. Myers, Dipole Moment of PH^+ and the Atomic Masses of ^{28}Si, ^{31}P by Comparing Cyclotron Frequencies of Two Ions Simultaneously Trapped in a Penning Trap, Phys. Rev. Lett. 100 (2008) 093002.

[149] M. Redshaw, B. J. Mount, E. G. Myers, Penning-trap measurement of the atomic masses of ^{18}O and ^{19}F with uncertainties 0.1 parts per 10^9, Phys. Rev. A 79 (2009) 012507.

[150] B. J. Mount, H. S. P. Müller, M. Redshaw, E. G. Myers, Mass of ^{17}O from Penning-trap mass spectrometry and molecular spectroscopy: A precision test of the Dunham-Watson model in carbon monoxide, Phys. Rev. A 81 (2010) 064501.

[151] R. Rana, M. Höcker, E. G. Myers, Atomic masses of strontium and ytterbium, Phys. Rev. A 86 (2012) 050502.

[152] S. L. Zafonte, Ph.D. thesis, University of Washington (2012).

[153] M. Schuh, F. Heiße, T. Eronen, J. Ketter, F. Köhler-Langes, S. Rau, T. Segal, W. Quint, S. Sturm, K. Blaum, accepted by Phys. Rev. A (2019).

[154] R. S. Van Dyck, F. L. Moore, D. L. Farnham, P. B. Schwinberg, Number dependency in the compensated Penning trap, Phys. Rev. A 40 (1989) 6308–6313.

[155] M. Schuh, Ph.D. thesis, Ruprecht-Karls University Heidelberg (2019).

[156] L. S. Brown, G. Gabrielse, Geonium theory: Physics of a single electron or ion in a Penning trap, Rev. Mod. Phys. 58 (1986) 233.

[157] J. Ketter, T. Eronen, M. Höcker, S. Streubel, K. Blaum, First-order perturbative calculation of the frequency-shifts caused by static cylindrically-symmetric electric and magnetic imperfections of a Penning trap, Int. J. Mass Spectrom. 358 (2014) 1 – 16.

[158] S. Rau, et al., in preparation.

[159] S. Sturm, I. Arapoglou, A. Egl, M. Höcker, S. Kraemer, T. Sailer, B. Tu, A. Weigel, R. Wolf, J. Crespo, K. Blaum, The ALPHATRAP experiment, Eur. Phys. J. Spec. Top. (2019) 1425.

[160] M. Bohman, A. Mooser, G. Schneider, N. Schön, M. Wiesinger, J. Harrington, T. Higuchi, H. Nagahama, C. Smorra, S. Sellner, K. Blaum, Y. Matsuda, W. Quint, J. Walz, S. Ulmer, Sympathetic cooling of protons and antiprotons with a common endcap Penning trap, J. Mod. Opt. 65 (5-6) (2018) 568.

[161] G. Gabrielse, Why Is Sideband Mass Spectrometry Possible with Ions in a Penning Trap?, Phys. Rev. Lett. 102 (2009) 172501.

Acknowledgment

Zuerst und am allermeisten möchte ich Gott dafür danken, dass ich sowohl die Möglichkeit als auch das Privileg geschenkt bekommen habe, meine Zeit mit dem Studium der Natur verbringen zu dürfen. Das ist eine der besten Entscheidungen meines Lebens. Ich bin sehr dankbar, dass ich bisher so viele gesegnete Situationen erleben durfte und es eine so erfüllende Zeit ist, seine Schöpfung zu studieren. Ich möchte Gott für seine große Gnade und Güte danken, dass er mich mit vielfältigen Talenten gesegnet hat, um diese zu seiner Ehre einzusetzen.

Ich möchte dir, Wolfgang, dafür danken, dass ich durch dich die Chance bekommen habe, in dieser einmaligen Gruppe und an diesem wunderbaren Experiment mitzuwirken. Danke, dass du jederzeit für die experimentellen oder auch organisatorischen Herausforderungen geholfen hast. Danke ebenfalls für dein immer offenes Ohr sowie die zahlreichen informativen Gespräche zu den verschiedensten Themen über Gott und die Welt.

Weiterhin möchte ich Selim Jochim danken, dass er sich bereit erklärt hat, diese Dissertation als Zweitgutachter zu begleiten.

Ich möchte mich bei dir, Klaus, ebenfalls herzlich bedanken, dass auch du mich die letzten vier Jahre stets begleitet hast. Danke, dass wir uns durch deinen Einsatz wirklich zu 100% auf die Forschung, welche uns erfüllt und große Freude bereitet, konzentrieren können. Es ist gut zu wissen, dass du für jedes Problem wortwörtlich zu jeder Tages- und Nachtzeit erreichbar bist. Danke für die vielen aufschlussreichen Gespräche und Anregungen in Bezug auf Paper, Vorträge und darüber hinaus.

Lieber Sven, ich möchte mich für deine exzellente Supervision am Experiment bedanken. Dein Überblick sowie die Gabe, Probleme zu identifizieren bevor sie auftreten, sind ein einzigartiger und unersetzbarer Beitrag für dieses Experiment. Weiterhin bin ich auch sehr dankbar, dass ich durch dich zu einem tieferen Verständnis phyikalischer Gesetzmäßigkeiten gekommen bin. Am meisten beeindruckt mich jedoch deine absolut demütige Art; ich glaube sie ist der Grundstein für unseren ausgzeichneten Teamspirit.

Danke Florian, dass du mich vom allerersten Tag an bis zum Ende hin so geduldig und liebevoll begleitet hast. Danke, dass ich mit dir über alle möglichen Fragen zum Experiment und darüber hinaus diskutieren durfte. Danke, für deine

passenden Intuitionen, welche das Experimiment beschleunigt haben. Für mich war es ideal, dass du mir die gesamte Zeit sowohl am Experiment als auch bei Vorträgen oder Papern mit Rat und Tat zur Seite gestanden hast.

Lieber Sascha, ich möchte dir für deine vielfältige Hilfe und Unterstüzung im Labor, bei Vorträgen und Papern ebenfalls danken. Ohne dich wäre die gemeinsame Zeit am Experiment nicht so erfolgreich geworden. Mit deinem klaren und scharfen Verstand haben wir so einige Klippen umsegelt. Danke für die vielen kritischen Fragen, welche zu einem tieferen Verständnis führten.

Explizit möchte ich mich noch einmal ganz herzlich bei euch dreien, Sven, Florian und Sascha, für die wirklich wundervolle Zeit über die letzten Jahre bedanken. Ich denke wir waren gemeinsam ein richtig gutes Team und haben uns in unseren Stärken und Schwächen perfekt ergänzt. Ich habe die Zusammenarbeit sehr genossen. Danke vielmals für die einmalige und geniale Zeit mit den ausgezeichneten Ergebnissen!

Darüber hinaus möchte ich mich gern bei Herrn Werth und der Proton g-Faktor Gruppe für die zahlreichen Gespräche während des Mittagessens über alle möglichen Themen bedanken. Ebenfalls geht mein Dank an die Heidelberger Fallenexperimentgruppen; eure Erfahrung hat uns weitergeholfen und unser Experiment verbessert.

Ich möchte weiterhin meiner Familie und Freunden für die Unterstüzung in allen Lebenslagen danken. Es tut gut zu wissen, dass ich jederzeit mit eurem Rückhalt und eurer Hilfsbereitschaft rechnen kann. Danke, dass ihr mich auf meinem bisherigen Weg immer begleitet und gefördert habt.

Schließlich möchte ich noch dir, liebe Carolin, von ganzem Herzen danken. Danke, dass du kompromisslos mit mir an jeden Ort der Welt gehst. Danke, dass du mir so häufig den Rücken freigehalten und mich in unzähligen Situationen immer wieder unterstützt hast. Deine Liebe motiviert mich und gibt mir die Kraft, wenn ich keine habe. Du bist für mich jeden Tag aufs Neue ein wirklich großer Segen. Danke, dass du uns schon ein so großes Geschenk gemacht hast, an dem wir uns jeden Tag erfreuen dürfen. Es ist wirklich wunderbar, dass es Junia gibt und sie uns immer wieder aufs Neue überrascht und unser Leben erfrischt. Wie aufregend wird es dann erst in Zukunft werden. Danke Carolin, dass es dich gibt und ich dich kennen darf! Danke, dass du mich so animmst und liebst wie ich bin!